UNIVERSITÀ DELLA CALABRIA

UNIVERSITA' DELLA CALABRIA

Dipartimento di Fisica

Dottorato di Ricerca in

Scienze e Tecnologie Fisiche, Chimiche e dei Materiali

CICLO

XXXII

TITOLO TESI

Radon measurement techniques in building materials and water using Italian and Ecuadorian samples

Settore Scientifico Disciplinare FIS/01

Coordinatore: Ch.ma Prof. ssa Gabriella Cipparrone

Firma Firma oscurata in base alle linee guida del Garante della privacy

Supervisore/Tutor: Ch.ma Prof. ssa Marcella Capua

Firma Firma oscurata in base alle linee guida del Garante della privacy

Dottoranda: Dott./ssa Jheny Orbe Ordóñez

Firma Firma oscurata in base alle linee guida del Garante della privacy

Abstract

Several studies have widely shown that there is a strict correlation between radon exposure and potential health hazard to the population. The indoor radon concentration depends on the radon exhalation from soil and building materials and radon in the domestic water supply. Accurate knowledge of the exhalation rate of building materials and radon concentration in drinking water plays an important role in reducing the risk for the population.

Detailed research is being carried out into the measurements of the exhalation rate of building materials and numerous publications are available. However, analysis of published results shows that a standard measurement protocol would be necessary and is not yet available.

As regards the assessment of radon gas content in source water, international protocols are available, however, the high dependence of measurements on numerous parameters, both environmental and instrumental, it still requires studies to choose the most suitable instrumentation and procedure in particular circumstances and in measurement campaigns.

This thesis presents the results of studies aimed at contributing to the realization of a protocol for measuring the radon exhalation rate in building materials. In addition, it presents the results of measurements of radon in water intended for human consumption under different experimental conditions. Standard instruments have been used for this purpose, such as scintillation chambers, gamma spectrometry, electrets and a radon chamber built in our laboratories. The emphasis will be on the work carried out with the radon chamber built for the research on the exhalation rate and adapted by us, for the first time, for radon gas concentration measurements in water.

The results obtained with the radon chamber are in excellent agreement with those obtained with the commercial instrumentation but the measurements with the chamber will allow a wide research activity on the dependence

of the measurements in water on different environmental parameters.

Of no less importance is the fact that the studies were conducted in parallel in Italy, in the physics department of the University of Calabria (UNICAL) and in the analogous laboratory of the physics department at the Escuela Superior Politécnica de Chimborazo (ESPOCH) in Riobamba, Ecuador, where a radon chamber twin to the Italian one was built.

Samples of Italian tuff were taken to the ESPOCH laboratoryfor a comparison of the measurements of the exhalation rate. In both laboratories exactly the same protocol was used, but each was equipped with an independent radon chamber and different instrumentation. Despite the different experimental and environmental circumstances, the results obtained are in excellent agreement with what was observed at UNICAL and confirm the quality of our protocol.

With our protocols were studied different samples: Italian and Ecuadorian building materials, commonly used in the construction of houses and buildings and water samples collected from wells and springs of the Calabria region in Italy and the Chimborazo province in Ecuador.

The results of the radon exhalation rate of the analyzed materials show a wide variability due to the different physical and chemical properties of the samples. The results range from the minimum detectable to 0.86 Bq kg^{-1} h^{-1} obtained with a sample of crushed Italian tuff measured with the closed chamber technique. The results, obtained using different detectors and techniques, show a satisfactory agreement.

The results of the measurements of the radon concentration in the Italian and Ecuadorian spring waters collected, compared to the reference value, indicated in the European Directive EURATOM 51/2013 dedicated to water intended for human consumption, show values well below 100 Bq l^{-1} except for a Calabrian source, San Giovanni in Fiore, with a concentration of 133 Bq l^{-1} measured with the closed chamber technique.

Protection from this important gas necessarily involves actions to prevent and inform the population, as also indicated by the recent Italian law 101/2020 implementing the EURATOM Directive 59/2013. To this end, the activities carried out with projects aimed at high school can, at the same time, bring young people closer to scientific research and a possible future in research, but also improve the knowledge of the dangers associated with

radon for these students and the surroundings in which they live. For this reason, the last chapter of this work briefly summarizes the activities of the INFN RadioLab project in which I have been able to participate in this three-year period and which has involved about 150 Calabrian and Ecuadorian students.

Abstract (Italiano)

Numerosi studi hanno dimostrato chiaramente la stretta correlazione tra l'esposizione al radon e il potenziale rischio per la salute. La principale causa di esposizione sono gli ambienti indoor, in questi, la concentrazione di radon può essere particolarmente importante poichè dipende dall'esalazione di radon dal suolo e dai materiali da costruzione e dal radon presente nella rete idrica domestica. Una misura accurata della concentrazione indoor ma anche del tasso di esalazione dei materiali da costruzione e della concentrazione di radon nell'acqua potabile, gioca un ruolo importante nella riduzione del rischio per la popolazione.

Ricerche dettagliate sulle misurazioni del tasso di esalazione dei materiali da costruzione sono disponibili in numerose pubblicazioni. Tuttavia, l'analisi dei risultati pubblicati mostra che un protocollo di misurazione standard sarebbe necessario e non è ancora disponibile.

Per quanto riguarda la valutazione del contenuto di gas radon nell'acqua sorgiva, sono disponibili protocolli internazionali, tuttavia, l'elevata dipendenza delle misure da numerosi parametri, sia ambientali che strumentali, richiede ancora studi per scegliere la strumentazione e la procedura più idonea in particolari circostanze e in campagne di misurazione.

Questa tesi presenta i risultati di studi volti a contribuire alla realizzazione di un protocollo per la misurazione del tasso di esalazione di radon nei materiali da costruzione. Inoltre, presenta i risultati delle misurazioni del radon nell'acqua destinata al consumo umano realizzate con diverse strumentazioni standard, come camere di scintillazione, spettrometria gamma, elettreti e una originale tecnica che utilizza una camera al radon costruita nei nostri laboratori. Particolare enfasi sarà data al lavoro svolto con la camera radon, costruita per misure del tasso di esalazione e da noi adattata, per la prima volta, per misure di concentrazione di gas radon in acqua.

I risultati ottenuti con la camera radon sono in ottimo accordo con quelli ottenuti con la strumentazione commerciale e misurazioni con la camera consentiranno un'ampia attività di ricerca sulla dipendenza delle misure da diversi parametri ambientali.

Non meno importante è il fatto che gli studi sono stati condotti in parallelo in Italia, nel dipartimento di fisica dell'Università della Calabria (UNICAL) e nell'analogo laboratorio del dipartimento di fisica presso la Escuela Superior Politécnica de Chimborazo (ESPOCH) a Riobamba , Ecuador, dove è stata costruita una camera radon gemella di quella italiana.

I campioni di tufo italiano sono stati portati al laboratorio ESPOCH per un confronto delle misurazioni del tasso di esalazione. In entrambi i laboratori è stato utilizzato esattamente lo stesso protocollo, ma ciascuno era dotato di una camera radon indipendente e di una strumentazione diversa. Nonostante le diverse circostanze sperimentali e ambientali, i risultati ottenuti sono in ottimo accordo con quanto osservato presso UNICAL e confermano la qualità del nostro protocollo.

Con i nostri protocolli sono stati studiati diversi campioni materiali da costruzione italiani ed ecuadoriani, comunemente usati nella costruzione di case ed edifici e campioni di acqua sorgiva raccolti in Italia in Calabria e nella provincia del Chimborazo in Ecuador.

I risultati del tasso di esalazione di radon dei materiali analizzati mostrano un'ampia variabilità dovuta alle diverse proprietà fisiche e chimiche dei campioni. Un tasso di esalazione importante, 0,86 Bq kg $^{-1}$ h $^{-1}$, si è ottenuto con un campione di tufo italiano frantumato e misurato in camera chiusa.

I risultati delle misurazioni della concentrazione di radon nelle acque sorgive italiane ed ecuadoriane raccolte, rispetto al valore di riferimento, indicato nella Direttiva EURATOM 51/2013 dedicata alle acque destinate al consumo umano, mostrano valori ben inferiori a 100 Bq l $^{-1}$ ad eccezione di una fonte calabrese, San Giovanni in Fiore, con una concentrazione di 133 Bq l $^{-1}$ misurata con la tecnica camera chiusa.

La protezione da questo importante gas passa necessariamente anche da azioni di prevenzione e informazione della popolazione, come anche indicato dalla recente legge italiana 101/2020 in attuazione della Direttiva EURATOM 59/2013. A questo scopo le attività svolta con progetti rivolti alle scuole possono, allo stesso tempo, avvicinare i giovani alla ricerca scientifica

ed ad un possibile futuro nella ricerca, ma anche migliorare la conoscenza dei pericoli associati al radon di questi studenti e dell'intorno in cui vivono. Per questa ragione l'ultimo capitolo di questo lavoro brevemente sintetizza le attività del progetto INFN RadioLab al quale ho potuto partecipare in questo triennio e che ha coinvolto con chiaro successo circa 150 giovani calabresi e ecuadoriani.

Contents

Introduction

Every day people are exposed to natural sources of ionizing radiation. Of all the radioisotopes contributing to natural background, radon is typically the major source of risk to human health, numerous studies show that radon is the second-largest cause of lung cancer after smoking. The gas is naturally present in most houses and working places, in negligible or important concentrations, depending on the characteristics of the soil on which the house is built, the building and decorative materials present in it and the indoor use of spring water. In particular, as regards building materials, it is important to know the radon exhalation power of these, to predict the contribution they will be able to give to indoor concentration even before they are used.

The control strategies recommended by international radioprotection organizations, incorporate in directives and laws, include the evaluation of the risk in homes and mitigation plans for cases that exceed the guidelines levels.

This thesis is in the field of Environmental Physics, in particular deals with radon gas concentration of activity measurements in water and exhalation rate of building materials, two important sources of radon indoors.

The two most popular techniques for the evaluation of the exhalation rate are the closed chamber and electret techniques. In the literature there are many studies on this and, in the report ISTISAN 17/2013, there is an interesting summary of many measurements publications, but, to date, a comparison between results is not simple because not all publications contain sufficient information on both the properties of the measured samples and the methods used. this study of the radon exhalation rate, using samples of Italian and Ecuadorian materials, wants to contribute to the realization of a protocol that allows to compare the results obtained in different laboratories and countries. In addition, it shows that measurements can be made in a relatively short time while keeping uncertainties under control and therefore proposes the use of the exhalation rate for the assessment of the contribution

to radon risk in building materials instead of the alpha index which by its nature cannot be the means of optimal evaluation.

The studies and protocols performed in Italy at UNICAL were tested in a twin laboratory in Ecuador at ESPOCH, using samples already studied in Italy. The results obtained are in excellent agreement.

Part of the research was devoted to improving knowledge of the radon concentration measurement techniques in water samples comparing four different techniques. The results will be useful to choose the most appropriate instrumentation in campaigns of monitoring of radon gas concentration in spring water (EURATOM Directive 2013/51). One of the techniques studied, uses the closed chamber built for the exhalation rate research, this original and not commercial chamber and technique has been tested during the first Italian intercomparison between measurements of radon concentration in water, this non-commercial technique is certainly promising in the field of research.

My research began in November 2016 at the Department of Physics of the Calabria University and was also conceived with the aim, not secondary, of contributing to the transfer of scientific knowledge to Ecuador. Part of the year 2018, I worked at the Faculty of Science of the Escuela Superior Politécnica de Chimborazo, Riobamba-Ecuador, accomplishing a twin laboratory of the existing at the UNICAL. Encouraging measurements of radon in water and building materials were made during this period.

In this thesis, after a brief introduction of the foundations of radon gas in Chapter 1, the theoretical assumptions of the measurement methods adopted and the samples studied are presented in the second chapter of this thesis. The results of the measurements of radon concentration in spring water and of the radon exhalation rate in Italian and Ecuadorian building materials, performed in the two laboratories, and the comparison of the measurements made in the laboratories using samples of Italian tuff, are presented in Chapters 3 and 4.

Knowledge by the population of the risk associated with this natural gas, the importance of measuring and research in general, can be obtained through actions of scientific dissemination. For this reason, part of my work has been devoted to scientific dissemination. It is important that young students are more familiar with the issues related to radioactivity in the environment and health protection. This is especially true in Ecuador, where the different

natural resources, including volcanoes, mining materials and water springs, have not yet been studied extensively in terms of the risks associated with radioactivity. Thanks to my association with the Istituto Nazionale di Fisica Nucleare (INFN), it was possible to successfully integrate a group of Ecuadorian high school students into the INFN national project RadioLab. A brief description of this activity is presented in the last chapter.

The aim of Radiolab is to introduce young people to scientific research dressing on the role of future researchers involved in issues related to radioactivity in the environment and using the radon case as an example. At the end of the thesis a brief description of the project, still in progress, is presented.

Chapter 1

Radon fundamentals

Introduction

This chapter briefly describes the main physical and chemical properties of radon, the mechanisms of release and transport from the earth's crust to the environments in which we live.

The second part of the chapter summarises the main recommendations of the international agencies and defines the variables of interest in this study.

1.1 Radon properties

The first two isotopes of radon were discovered in 1900: the isotope 220 (thoron) by R.B. Owens and E. Rutherford, and the isotope 222 (radon) by F.E. Dorn. In 1903 André L. Debierne discovered the isotope 219 (actinon) produced by the decay of actinium. Their respective half lives are 55.6 s, 3.82 d, and 3.96 s.

Radon is a unique natural gas, noble and radioactive in all of its isotopes. Radon is denser than air and fairly soluble in water, solubility decreases with increasing temperature (0 ^oC is 53 cm^3 radon/100 cm^3 water, at 100 ^oC is 11 cm^3 radon/100 cm^3 water). At standard temperature and pressure the radon density is 9.73 kg m^{-3}[1].

The radioactive series of radon, thoron and actinon are shown in Figure (1.1). The isotope 222, of interest of this thesis, belongs to the decay chain of uranium-238 and is the immediate decay product of radium-226. The first descendent of radon is polonium-218, produced by alpha decay. In general,

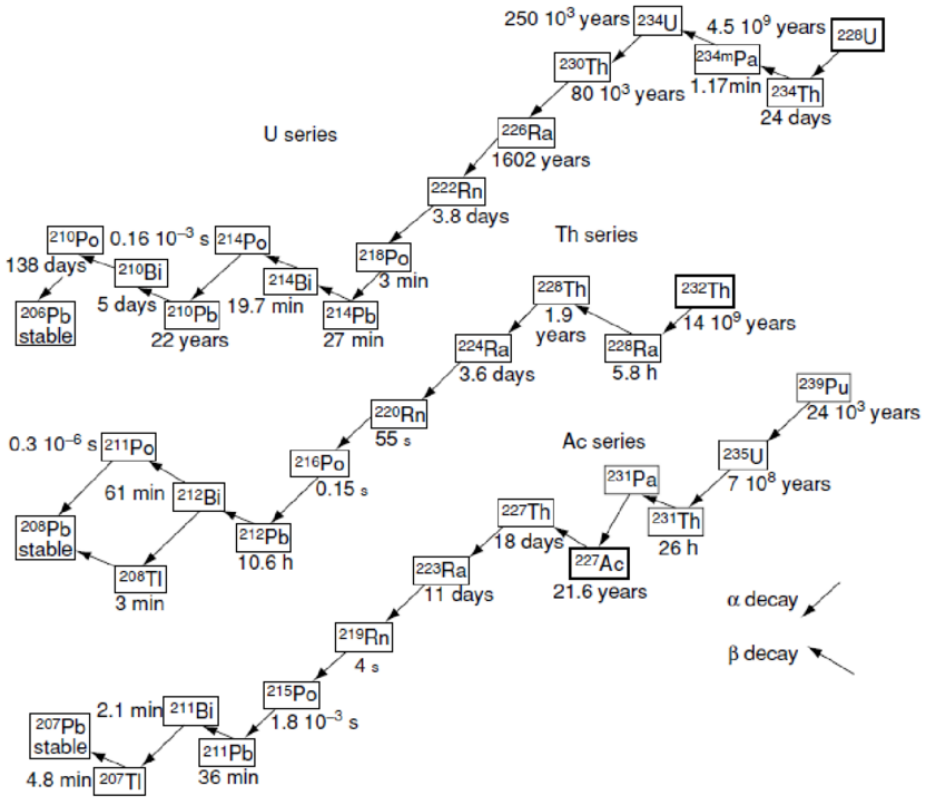

Figure 1.1: Uranium, thorium and actinium series [2].

the relative importance of the three radon isotopes increases with their mean lives and relative abundance. ^{219}Rn is the shortest lived, and is always produced in much smaller amounts than is ^{222}Rn, since the natural $^{235}U/^{238}U$ ratio of these ultimate progenitors is 0.00719. Hence ^{219}Rn is measured less frequently. ^{220}Rn too is short lived relative to ^{222}Rn and consequently moves a much smaller distance from its source than does ^{222}Rn. In air, for a diffusion constant, D, of 0.1 cm^2 s^{-1}, the mean distance of diffusive motion over a mean life $\sqrt{D\tau}$ is 2.2 m for ^{222}Rn and 0.029 m for ^{220}Rn. For this reason ^{222}Rn is by far the nuclide more studied and of radioprotection interest and ^{220}Rn provides, depending on the measurement technique, only a background during ^{222}Rn detection. Exceptionally high Th/U ratios, however, can lead to greatly enhanced ^{220}Rn relative to ^{222}Rn.

1.2 Release and transport of radon

Most radon that is produced by the decay of radium never escapes from the mineral in which it is born; rather usually it is wedged tightly in place within the crystal lattice for the few days until it in turn decays. The small fraction of radon escaping from the miner enters the pores, filled with air or water (emitted fraction).

Conservation of momentum reveals that emission of an alpha particle with energy of 4.78 MeV by ^{226}Ra gives the ^{222}Rn daughter nucleus a recoil energy of 86 keV (sufficient to move the recoiling radon through 26 nm of SiO_2 [3]). The possibility for escape is direct ejection from the mineral grain of the radon atom by recoil. In particular, if the radio atom is located near the edge of the grain, see Figure (1.2), the produced radon will transfer, thanks to recoil energy, into an adjacent grain or into a pore. If the pore space contains water, the ejected recoil most often will be brought to rest in the liquid as sketched in the right part of Figure (1.2). The radon atom is then free to diffuse from the water or be transported by it.

About the pore, if the pores are filled with water the radon will be dissolved there. If the pore is only partially filled with water the partition between the air and water is described by Henry's law in terms of the Oswald coefficient, K:

$$K = \frac{C_w}{C_a} \tag{1.1}$$

where C_w and C_a are the radon concentrations (Bq m^{-3}) in the water and air, respectively. The Oswald coefficient varies inversely with temperature.

Another possibility, shown in the left part of Figure (1.2), is that the interstitial space is dry (filled only with soil gas) and not wide enough to stop the recoiling radon. In this case, it enters a neighboring grain- apparently immobilizing itself. It is however, less isolated than if it failed to exit its grain of origin, the reason being that radiation damage extends to it from where it entered its new grain. This damage turns out to be etchable by exposure to water. Hence, if the originally dry grains become wet before the radon has decayed, it can be released into the interstitial space.

The *emanation fraction* is defined as the fraction of radon that reaches the pores. For typical soils or bedrock, the emanation fraction can range

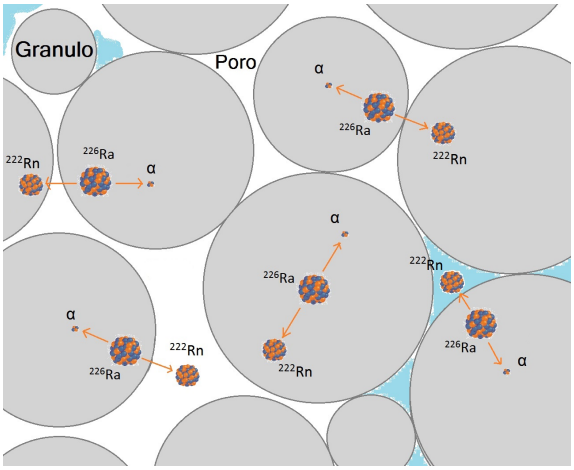

Figure 1.2: Radon release mechanisms from a mineral grains.

from 5% to 50% [4].

The main transport mechanisms are diffusion and forced flow. Diffusion is the process whereby atoms migrate toward regions with lower concentrations. The main reason for this is that the radon atoms are confined within a small volume defined by the pore space between the soil grains. Thus, radon will preferentially diffuse toward regions that have lower concentrations, such as caves, tunnels, buildings, and the atmosphere. Diffusion inevitably occurs, even though its extend may be limited.

Forced flow depends on pressure gradients, which may or may not be present in a given situation. In any such case diffusive effects are superimposed on those of pressure gradients. Air will flow toward locations with lower pressure, and changes in atmospheric pressure can force air into or out of the ground. Very often, the air inside a building is warmer than air in the soil that is in contact with the building. This temperature difference causes a pressure gradient that draws air containing high concentrations of radon into the structure. Wind as well as airflow from a fan, furnace, or fireplace can also reduce pressures inside a building, compared with the pressures in the soil adjacent to the building foundation. These processes constitute the primary reason that radon enters and may be present in buildings at higher concentrations than in ambient air.

A constituent of the soil gas such as radon flows in a direction opposite to that of the increasing concentration gradient (Fick's Law). If the diffusive

flow is upward in the z-direction:

$$J_d = -D\frac{dC}{dz}$$

Where J_d is the diffusion current density, D is the bulk diffusion coefficient, and C is the concentration of ^{222}Rn in the interstitial space. If there is a fluid current density J_f also in the positive z-direction, then $J_f = Cv$, where v is the transport velocity. The steady-state equation for a semi-infinite, homogeneous, porous medium is [5]:

$$\frac{D}{\epsilon}\frac{d^2C}{dz^2} - \frac{1}{\epsilon}\frac{d(vC)}{dz} - \lambda_{Rn}C + \phi = 0 \tag{1.2}$$

Where ϵ is the soil porosity, λ_{Rn} is the decay constant of ^{222}Rn, and ϕ is the production rate per unit volume of ^{222}Rn atoms that are free to migrate in the interstitial space. The terms in Equation (1.2) represent, in order, diffusion, flow, decay, and production. For flow by molecular diffusion alone, and with boundary conditions C = 0 at z = 0 and $C = \frac{\phi}{\lambda_{Rn}}$ at z = - ∞, the following solution of Equation (1.2) is obtained:

$$C = \frac{\phi}{\lambda_{Rn}}\{1 - exp[(\frac{\epsilon\lambda_{Rn}}{D})^{1/z}]\} \tag{1.3}$$

This shows that the concentration increases with depth. Molecular diffusion as a significant transport mechanism is limited to the first few meters of surface soil [6].

Once the solution of Equation (1.2) is found for a specified form of the transport velocity v, the total ^{222}Rn current density J in the soil is:

$$J = -D\frac{dC}{dz} + Cv \tag{1.4}$$

The dependence of v on z in fluid flow is found by application of Darcy's Law $v = -(\kappa/\eta)dp/dz$ where p is the pressure, κ is the soil permeability, and η is the dynamic viscosity of the fluid. Equations (1.2) and (1.4) furnish the points of departure for models relating the physical properties of soils to transport that is the result of both molecular diffusion and a pressure-induced flow.

Radon diffusion rates in air and water are very different. Table (1.1) shows the diffusion constant D in water is lower by a factor of 10^4. There is a mean distance of motion of a radon isotope before it disappears by decay ($\sqrt{D\tau}$). Thus the average ^{222}Rn atom moves about 1.6 m in dry porous soil, but only 1.6 cm in water-saturated soil.

Medium	**Mean distance**		**Diffusion constant**
	^{222}Rn (cm)	**^{220}Rn (cm)**	**cm^2 s $^{-1}$**
Air	220	2.85	10^{-1}
Porous soil	155	2.0	5.10^{-2}
Water	2.2	0.0285	10^{-5}
Saturated porous soil	1.55	0.020	5.10^{-6}

Table 1.1: Mean diffusion distances of radon and thoron in different media [3].

The mean diffusion distances given in Table (1.1) are important in setting limits on the effective motion of radon and thoron in the absence of special transport mechanisms. Thus the radon inputs to the foundations of homes come primarily from soil within 1 or 2 meters of the house - a very local source [3].

Diffusive transport in soil and rock

Diffusive motion in the ground is in air and water, but is controlled by the extent of open, connected porosity in the soil and rock. In general higher porosity enables more extensive diffusive transport; but it is critical to consider only that fraction of the pore space that allows through motion. Most porosity in soil is interconnected; but in rocks that is not necessarily true. For a group of 32 soils that extend from clays to silty sands, values of D ranged from 0.005 to 0.062 cm^2 s^{-1}, with an average of 0.03 [7].

Forced transport of radon in soil and rock

Pressure gradients can cause flow of the gas or liquid in interstitial space in the earth, the ease of such flow being given by the hydraulic permeability:

$$K = \eta \frac{dV/dt}{A(dP/dx)} \tag{1.5}$$

Where η is the viscosity, $(dV/dt)/A$ the volume moved per unit time and per unit area, and dP/dx the pressure gradient. K is in units of to the square of the length. Table (1.2) indicates values for hydraulic permeabilities.

Substance	**Permeability range (cm^2)**
Black slate powder	$4.9.10^{-10}$ - $1.2.10^{-9}$
Silica powder	$1.3.10^{-10}$ - $5.1.10^{-10}$
Sand (loose beds)	$2.0.10^{-7}$ - $1.8.10^{-6}$
Soils	$2.9.10^{-9}$ - $1.4.10^{-7}$
Sandstone	$5.0.10^{-12}$ - $3.0.10^{-8}$
Limestone, dolomite	$2.0.10^{-11}$ - $4.5.10^{-10}$
Brick	$4.8.10^{-11}$ - $2.2.10^{-9}$
Bituminous concrete	$1.0.10^{-9}$ - $2.3.10^{-7}$
Cork board	$3.3.10^{-6}$ - $1.5.10^{-5}$
Fiber glass	$2.4.10^{-7}$ - $5.1.10^{-7}$

Table 1.2: Representative values of hydraulic permeability [3].

Mechanisms of forced transport in the earth

The mechanisms in the earth that might produce gradients and thereby, effect radon flow, differ depending on the geophysical and geochemical phenomena: earthquakes, volcanic eruptions, oil prospecting and uranium prospecting.

Three main categories are gas emission, stresses, and fluid convection. Gases can be released by oil deposits [8], and they can be generated and pressurized by hot regions such as volcanos. Stress can be generated by the build-up of strains that precede earthquakes [9] and volcanic eruptions, and the stress gradients in turn can encourage fluid flow in the earth.

Fluid convection, could produce flows if there were sufficiently steep geothermal gradients and high enough permeabilities [10]. Such flows could deliver signals from uranium deposits from greater depths than would allow detection of ore solely by diffusion of radon. Here again volcanic effects (in this case thermal) could reveal impending activity.

A fourth contributor to pressure-induced flow is atmospheric pumping in the near surface soil by the pressure fluctuations that are associated with weather systems [11]. Track-based radon measurements are normally taken over weeks in order to average and thus minimize such effects.

Permeability through materials

The permeability of radon through materials are of interest for two primary reasons. One reason is the obvious need for barriers to seal homes against the entrance of radon [12]. The second reason is less obvious, the use of membrane barriers to keep all other alpha emitting isotopes except radon out of a detector air space, so that ^{222}Rn can be measured by itself [13].

Table (1.3) shows permeabilities, k, for plastic sheets and caulking compounds. A delay time ($\tau_m = \frac{V\delta}{kA}$) is given for radon entering an air space of volume V through a membrane of area A and thickness δ.

Substance	**Permeability**	**Delay time***
	(10^{-8} cm^2 s^{-1})	**days**
Membrane materials		
Cellulose acetate (cellit-T)	0.75	19
Cellolose nitrate	12.5	1.1
Celgard (porous filter impregnated with silicone oil)	150	0.096
Dimethylsiloxane-bisphenol polycarbonate copolymer (MEM-213)	125-840	0.017-0.113
Fiberglass	450	0.032
Hydrate cellulos (cellophane)	0.97	15
Polycarbonate	0.38	38
(Makrofol G)	2.4	6
(Makrofol KG)	0.55	6
Polyester	0.20	26
Polyethylene terephthalate (Mylar)	0.084	170
Melinex-0	0.30	48
Polyethylene	0.34	42
	7.8	1.8
2 ^{o} C	2.8	5.1
23 ^{o} C	5.5	2.6
43 ^{o} C	16.5	0.88
Polyvinylchloride	5.0	2.9
(Dom pak)	0.58	25
(Folpak)	0.61	23
Rubber natural	635	0.022
Polymethyl methacrylate (plexiglas)	0.011	
Caulking compounds		
Acrylic latex (GE)	0.4	36
Polyuretane (Bondex)	80	0.18
Silicone (GE silpruf)	140	0.1

* V δ /A = 0.0123 cm^2 assumed

Table 1.3: Radon permeabilities and transit times for various materials [3, 14].

Radon originates from radium decay in soil grains; a small fraction of it is freed to move through the pore spaces into the atmosphere over land.

Homes, because they lie at the interface between the soil and the continental atmosphere, have radon concentrations that are intermediate between those of the soil gas and the free atmosphere. Table (1.4) gives rough representative numbers for the concentrations of radon at various locations.

Location	**Concentration (atoms cm^{-3})**
Air over oceans	0.04
Air near the earth's surface	4
Typical home en the US	20
Soil gas	20000
Interior of typical mineral	500000

Table 1.4: Typical ^{222}Rn concentration [3].

The heterogeneous distribution of uranium has implications for the processes responsible for the release of radon. These are aided by uranium and radium being close to mineral surface.

1.3 Radon risk on human health

The first four short-lived descendants of radon ^{218}Po, ^{214}Pb, ^{214}Bi, and ^{214}Po (radon decay products) are all with a short half-lives ranging from a fraction of a second to 27 min. Indoors, some of these decay products come into contact with surfaces and are removed from the air by a process called plate-out. The rest of the decay products remain suspended in air as free atoms (unattached) or combined with other aerosols (attached).

To calculate the exposition to radon, the equilibrium factor F is used [15]. Indoor radon and descendants are in disequilibrium fraction, ranging between 0 and 1 depending on the radon entrance and removal equilibrium. Studies on the attached and free radon daughters allow the calculation of F, defined as the activity of the short half-life daughter over the activity, assuming equilibrium between radon and descendants in indoor air:

$$F = \frac{C_{eq}}{C_o} \tag{1.6}$$

In addition, the total energy that would be released by alpha particles when all the short-lived atoms decayed completely is defined as potential alpha energy (PAE), and the concentration in air (PAEC), is measured in

units of energy per unit volume of air.

The development of a PAEC from indoor radon concentration depends on air movement and aerosol conditions within a room. PAEC can depend on whether the radon entered a room from soil or from water during bathing. The relationship between indoor radon concentration and PAEC is expressed in terms of the equilibrium ratio (ER). For a room without any depletion of radon or plate-out of decay products, ER = 1.0. In domestic environments, ER ranges from 0.3 to 0.7 with a nominal value of 0.4 [16]. The alpha-particle dose to lung tissues depends on PAEC and on the time that a person spends in a given location. A combination of PAEC and time is a measure of exposure expressed in joule-seconds per cubic meter.

There is a direct implication between exposition to radiation and health effects in humans. For example, excess cancers have been observed in a cohort of survivors of the atomic bomb blasts in Japan [16]. A relationship between lung cancer and inhalation of radon decay products has been demonstrated in underground miners [17]. Epidemiological studies suggest that inhalation of radon decay products in domestic environments could also be a cause of lung cancer [18, 19, 20, 21]. Although the studies do not specifically identify health effects at low doses, there is compelling circumstantial evidence that they occur.

Under ambient conditions of low dose and low dose rate, any health effects associated with exposure to radon in air or water can be expected to occur from the passage of single alpha particles through individual cells. Any given cell is hit only once or not at all. An increase in exposure increases the number of cells that are hit, but it will not affect the primary damage experienced by each cell. Therefore, the initial events depend linearly on exposure or dose.

Exposed cells experience local damage in the form of DNA breaks and the products of reactive oxygen. The damage is metabolized by cellular-repair systems, and some fraction of it results in permanent genetic changes. Those changes can lead to the development of cancers; a cancer usually originates in a single transformed cell.

Risk projection models have been developed to predict the risk in situations where direct evidence is not available (National Research Council 1999; 1990a). The nature of the exposure to indoor radon, the kinds of DNA damage inflicted by alpha particles, and the extent of repair are consistent with the absence of a threshold for cancer induction. The preferred model is

a straight line that reaches zero risk only when the dose or exposure is zero; it is referred to as the linear no-threshold (LNT) model.

Absorbed dose from indoor radon

A person in a room will inhale radon decay products that are suspended in air. Some activity can deposit and accumulate in the respiratory airways, depending on breathing patterns and the aerodynamic size of the particles with which the decay products are associated. Because of the short half-lives, the radon decay products that are deposited in the lung will almost certainly decay completely in the lung. The radiations emitted within the lung during these decays can deposit energy in the body. However, this radioactivity is very near the lung epithelium, so alpha particles in particular can transfer copious amounts of energy to vulnerable cells. That is why radon decay products are characterized in terms of PAEC.

Radon gas itself is also inhaled. Most of it is exhaled immediately and therefore does not accumulate in the respiratory system, as do radon decay products. Because the radon does not get close to radiosensitive cells, the absorbed dose from alpha particles is small. However, some of the radon that reaches the interior region of the lung is transferred to blood and dispersed throughout the body. Radon and the decay products formed inside the body can deliver a radiation dose to tissues and organs.

On some occasions, water is consumed immediately after leaving the faucet before its radon is released into the air. This water goes directly to the stomach. Before the ingested water leaves the stomach, some of the dissolved radon can diffuse into and through the stomach wall. During that process, the radon passes next to stem or progenitor cells that are radiosensitive. These cells can receive a radiation dose from alpha particles emitted by radon and decay products that are created in the stomach wall. After passing through the wall, radon and decay products are absorbed in blood and transported throughout the body, where they can deliver a dose to other organs.

Ingested water eventually passes through the stomach into the small intestine, where the remaining radon and decay products are released from the water and transferred to blood. They then circulate within the body; most are released from the blood into the lung and exhaled, but some remain in the blood and accumulate in organs and tissues, which receive an absorbed dose from alpha, beta, and gamma radiation.

1.3.1 Definitions related to radon regulations and standards

Annual effective dose

In many cases the measurement of radon gas activity concentration is directly used to control indoor and workplace radon levels. One way of calculating the annual effective dose from inhaling radon, as suggested in ICRP 137 and adopted by Italian low 101/2020, is as follows:

$$Effective_{dose} = CtD \tag{1.7}$$

where C is the average radon concentration (in Bq m^{-3}) measured in the indoor environment of interest, t is the time spent in that place and D is the dose coefficient. ICRP recommends a dose coefficient of 3 mSv per mJ h m^{-3} in the most circumstances that, using the equilibrium factor of 0.4, corresponds to 6.7 x 10^{-6} mSv per Bq h m^{-3}; for work indoors involving substantial physical activity, ICRP recommends 1.4 x 10^{-5} mSv per Bq h m^{-3}.

Gamma and alpha activity index

Natural radionuclides present in building materials used for the construction of indoor spaces (houses, workplaces, etc.) can cause exposure, internal and/or external to radiation. In particular, the materials derived from rock and soil contain mainly natural radionuclides of the uranium (^{238}U) and thorium (^{232}Th) series, and the radioactive isotope of potassium (^{40}K). The external exposure is caused by direct gamma radiation. The internal exposure is caused by the inhalation of radon (^{222}Rn), thoron (^{220}Rn) and their short lived decay products.

Controls on the external exposure due to building materials, in order to restrict the highest individual exposure, can be based on the dose criterion [22]. Effective dose exceeding the dose criterion of 1 mSv y^{-1} should be taken into account in terms of radiation protection. The activity concentration index, also known as the gamma activity index is defined as [22]:

$$I_\gamma = \frac{C_{Ra}}{300} + \frac{C_{Th}}{200} + \frac{C_K}{3000} \tag{1.8}$$

where C_{Ra} C_{Th} and C_K are the activity concentrations in Bq kg^{-1} of the radionuclides (^{226}Ra, ^{232}Th and ^{40}K)in the building material.

An index lower than one corresponds to an annual effective dose less than or equal to 1 mSv.

The factors used for a dose of 0.3 mSv are 121 Bq kg^{-1}, 101 Bq kg^{-1} and 1390 Bq kg^{-1} for radium, thorium and potassium, respectively.

The internal exposure can be evaluated using the alpha index, an index dealing with the assessment of the excess alpha radiation due to radon inhalation originating from building materials. The index is defined as [23]

$$I_\alpha = \frac{C_{Ra}}{200} \tag{1.9}$$

Where C_{Ra} is the activity concentration of ^{226}Ra in Bq kg^{-1} in the building material.

When the radium activity concentration of a building material exceeds the value of 200 Bq kg^{-1}, it is possible that the radon exhalation from this material could cause indoor radon concentrations exceeding 200 Bq m^{-3}. On the contrary, when the ^{226}Ra activity concentration is below 100 Bq Kg^{-1} it is unlikely that the radon exhalation from the building materials could cause indoor radon concentrations exceeding 200 Bq m^{-3} [24, 25].

The recommended exemption level and recommended upper level for ^{226}Ra activity concentration are 100 Bq Kg^{-1} and 200 Bq Kg^{-1}, respectively, in building materials as suggested by the Radiation Protection Authorities in Denmark, Finland, Iceland, Norway and Sweden [26, 27].

1.4 International Radioprotection Agencies and Italian laws

The protection of living beings from the harmful effects produced by ionizing radiation, in particular for humans, is a subject that involves international organizations dealing with radiation protection. The main organizations are:

The International Commission of Radiological Protection (ICRP), constituted in 1928 under the name of the International Commission for the protection against X-rays and radio. This Commission is a non-governmental organization, but its scientific recommendations are accepted by all international organizations and adopted by the official regulations of all the States

that carry out nuclear activities. The mission of the organization is to provide recommendations and guidance on radiological protection concerning ionizing radiation.

The International Atomic Energy Agency (IAEA), inter- governmental nuclear agency, created by the United Nations in 1957. The headquarters of the Agency is in Vienna, and 140 states form part of it, according to data from 2006. Its tasks are very broad within the field of energy nuclear, such as: research and development, holding scientific conferences, control over the peaceful uses of fissile materials and formulation of recommendations on nuclear safety and radiation protection.

The Nuclear Energy Agency (NEA), was created within the Organization for Economic Cooperation and Development (OECD) in 1957. It is comprised of 28 States, including 21 European States, as well as Canada, the United States, Japan, Korea , Mexico, Australia and New Zealand; its headquarters is in Paris. Within the Agency there are four technical directions: science and nuclear techniques; technological development; nuclear security; radiological protection and radioactive waste management.

The European Nuclear Energy Community (EURATOM), now integrated within the European Union, today cover a large variety of areas associated with nuclear power and ionising radiation and also establishes a regulation on radiation protection and Directive for the States of the Union.

In particular:
The **EURATOM Directive 2013/59** [28] establishes uniform basic safety standards for the protection of the health of individuals subject to occupational, medical and public exposures against the dangers arising from ionizing radiation.

The EURATOM Directive 2013/59, in Article 54(1)and Article 74(1) recommends the member states to establish national reference levels for indoor radon concentrations in workplaces and residences. The reference levels for the annual average activity concentration in air shall not be higher than 300 Bq m^{-3} unless it is warranted by national prevailing circumstances.

In addition, the Directive EURATOM 2013/59 in Article 103(1) recommends the members states to establish a national action plan addressing long-term risks from radon exposures in dwellings, buildings with public access and workplaces for any source of radon ingress, whether from soil, building

materials or water. The action plan shall take into account the issues set out in Annex XVIII and be updated on a regular basis.

For building materials, Article 75(2) of the Directive EURATOM 2013/59 suggests identifying materials of concern from the point of view of radiological protection, taking into account the indicative list of materials in Annex XIII regarding their gamma radiation emitted, which is detailed below:
1. Natural materials
(a) Alum-shale.
(b) Building materials or additives of natural igneous origin, such as: granitoides (granites, syenite and orthogneiss); porphyries; tuff; pozzolana (pozzolanic ash); lava.
2. Materials incorporating residues from industries processing naturally-occurring radioactive material, such as: fly ash; phosphogypsum; phosphorus slag; tin slag; copper slag; red mud (residue from aluminium production); residues from steel production.

Article 75 (2b) of the Directive EURATOM 2013/59 provides for determining the activity concentration index for the gamma radiation emitted by building materials (gamma index), taking into consideration that the reference level applying to indoor external exposure to gamma radiation emitted by building materials, in addition to outdoor external exposure, shall be 1 mSv per year (article 75 (1)). The calculation formula is described in annex VIII of the Directive.

The **EURATOM Directive 2013/51** [29] establishes requirements for the protection of the health of the population with regard to radioactive substances present in water intended for human consumption. With regard to radon, the directive in Annex I recommends a parametric value of 100 Bq l^{-1} for water intended for human consumption.

Member States may set a level for radon which is judged inappropriate to be exceeded and below which optimization of protection should be continued, without compromising water supply on a national or regional scale. The level set by a Member State may be higher than 100 Bq/l but lower than 1000 Bq/l. In order to simplify national legislation, Member States may choose to adjust the parametric value to this level. Remedial action is deemed to be justified on radiological protection grounds, without further consideration, where radon concentrations exceed 1000 Bq/l.

There are requirements in the EURATOM Directive 2013/51 regarding

detection limit and sampling frequency from drinking water supplies. The chosen radon measurement technique has to be capable of measuring activity concentrations with the following limit of detection: The limit of detection for radon is 10% of its reference value of 100 Bq l^{-1}, which is 10 Bq l^{-1}.

The annual sampling frequency and number of samples should be defined by Member states but they depend on water volume distributed or produced each day within a supply zone. The Directive 2013/51 adds that the number of samples should be distributed equally in time and location as much as possible.

In Annex II, imposes on the regions the elaboration and implementation of a program to control the concentration levels of radon in water intended for human consumption coming totally or partially from underground sources. The control program should collect information about the geological and hydrological characteristics of the area, radioactivity of the soil and all the useful information for the identification of areas with possible high levels of radon activity concentration in water. Italy, through national law impose a parametric value of radon in water of 100 Bq l^{-1}.

In Italy, although the law regarding application on Directive 59/2013 is still in preparation, the EURATOM Directive 2013/51 has became law in 2016 (DL 28/2016) [30].

The Environmental Protection Agency (EPA), EPA is an independent agency of the United States federal government for environmental protection. The program, about radiation protection, has various project groups to protect the public from radiation and proposed regulations to reduce the public health risks from radon on November 2, 1999 in the **Federal Register (64 FR 59246)** [31].

The standards apply only to community water systems that regularly serve 25 or more people and that use ground water or mixed ground and surface water (e.g., systems serving homes, apartments, and trailer parks). They do not apply to systems that rely on surface water where radon levels in the water are very low. They also do not apply to private wells, because EPA does not regulate them.

The proposal provides states flexibility in how to limit exposure to radon by allowing them to focus their efforts on the greatest radon risks (those in indoor air) while also reducing the risks from radon in drinking water.

First Option:
States can choose to develop enhanced state programs to address the health risks from radon in indoor air, known as Multimedia Mitigation (MMM) programs, while individual water systems reduce radon levels in drinking water to 4000 pCi/L (148 Bq l^{-1}) or lower (Alternative Maximum Contaminant Level AMCL).

Second Option:
If a state chooses not to develop an MMM program, individual water systems in that state would be required to either reduce radon in their system's drinking water to 300 pCi l^{-1} (11 Bq l^{-1}) (Maximum Contaminant Level MCL) or develop individual local MMM programs and reduce levels in drinking water to 4000 pCi l^{-1} (148 Bq l^{-1}.

The proposed regulation identifies four criteria that MMM program plans would be required to meet to be approved by EPA:
1)Public involvement in the development of the MMM plan;
2)Quantitative goals for reducing radon in existing and new homes;
3)Strategies for achieving these quantitative goals;
4)A plan for tracking and reporting results.

Exceeding the highest alternative maximum contaminant level might result in elevated health risks from indoor radon (radon escaping from water and into the indoor air) so mitigation is needed in the places concerned.

The World Health Organization(WHO)), the World Health Organization reference level for radon concentration in indoor air is 100 Bq m $^{-3}$ in dwellings. If this level cannot be reached under prevailing country specific conditions, the level should not exceed 300 Bq m $^{-3}$, corresponding to an annual dose of approximately 10 mSv (WHO, 2009).

The third edition of the World Health Organization's (WHO) Guidelines for drinking-water quality (Geneva, 2008) [32] in the chapter 9, provide criteria with which to assess the safety of drinking water with respect to its radionuclide content. In relation to radon, this indicates that radon in drinking-water supplies controls should be implemented if the radon concentration of drinking-water for public water supplies exceeds 100 Bq l^{-1}.

Any new, especially public, drinking-water supply using groundwater should be tested prior to being used for general consumption. If the radon

concentration exceeds 100 Bq l^{-1}, treatment of the water source should be undertaken to reduce the radon levels. Appropriate treatments include air stripping, aeration systems or for small water supplies activated carbon adsorption. If there are significant amounts of radon-producing minerals around the water source, then it may be appropriate for larger drinking water supplies to test for radon concentration periodically, for example, every 5 years.

However, in the current publication of the drinking water guidelines radon guidance level is missing and no other concrete guidance level is given (WHO, 2011) [33].

Chapter 2

Sampling and methods

Introduction

One of the main objectives of this thesis is the study of the best procedure to measure the concentration of radon gas in water and building materials, taking into account the requirements of the new European directives described in the Section (1.4). The research activities have been carried out in the Ionizing Radiation laboratory of the Calabria University (IRL), in Italy. Further studies has been performed in the Nuclear Techniques laboratory of the Escuela Superior Politécnica de Chimborazo (NTL), in Ecuador, where a twin-laboratory of IRL has been realized by T. Tene [34] and myself in the years 2017-2018. During my Ph.D., I spent eight months in Ecuador in order to perform measurements and testing the new laboratory.

This chapter presents the theoretical approach and the experimental techniques at the bases of radon measurements in water and building materials used in this study. A description of the instrumentation used in IRL and NTL laboratories is reported in Section (2.1), while details of the samples of Italian and Ecuadorian building materials that have been analyzed and the techniques studied are described in Section (2.2). The Section (2.3) presents the four techniques for measuring the concentration of radon in spring water samples, describes the study areas monitored in the Calabria region of Italy and in the Chimborazo province of Ecuador.

2.1 Instrumentation

2.1.1 Scintillation cells

The Lucas scintillation cell [35, 36] is an airtight aluminum cylinder that has a transparent quartz window coated with a tin oxide at one end and two swagelok connectors on the other side to pump the sample of air in the cell. The interior of the cylinder is lined with silver activated zinc sulfide, an alpha sensitive scintillating material. If the cell is filled with a sample of air containing radon, when the alpha particle due to radon decay hits the cell wall, photons for scintillation can be produced. The quartz window can be interfaced with a photomultiplier to count the photons produced by scintillation. The cells used in this work are produced by Pylon Electronics [37] and the equipment for the counting is a Pylon AB-5 counter [38] equipped with a pump, adjustable from 0 to 3 liters min^{-1}, to force air into the cell .

The six cells used in this thesis to mesure radon in water have a volume of approximately 270 ml (Pylon model 300A), a maximum background of 1 cpm, nominal counting efficiency of 0.76 $\pm$ 0.02 cpm dpm^{-1} and sensitivity of 0.037 cpm Bq^{-1} m^3 [37]. The sensitivity of the cells available in the laboratory varies between 0.030 and 0.035 cpm Bq^{-1} m^3 with an uncertainty of less than 10%.

A particular Pylon scintillation cell is the Continuous Passive Radon Detector (CPRD). The cell was used to measure radon concentration in air inside the closed chamber and in the laboratory. The CPRD is used with the Pylon model AB-5 portable radiation monitor to measure radon gas concentration with a lowerest detection limit (LDL) of 24.8 $Bq^{-1}m^{-3}$. The CPRD is an aluminum cylinder with four small openings at one end and completely opened at the other end. The four small openings have a light-proof polyurethane foam barrier and the open end fits the AB-5's counter. Air diffuses into CPRD spontaneously, thanks to the foam barrier, The CPRD is not affected by humidity, dust or changes in temperature. The CPRD sensitivity is 0.041 cpm $Bq^{-1}m^3$, it has an activity volume of 272 ml, maximum background of 0.75 cpm and a length of 15.2 cm [39].

The last calibration of AB-5 and cells has been effectuated in June 2018.

2.1.2 Solid state alpha detector

A soil state alpha detector incorporated into the RAD7 [40] continuous monitor manufactured by Durridge Company was used for radon measurements in air and water in Ecuador. The RAD7's internal cell is a 0.7 liter hemisphere, coated on the inside with an electrical conductor. An Ion-implanted, Planar, Silicon alpha detector is at the center of the hemisphere. The high voltage power circuit charges the inside conductor to a potential of 2000 to 2500 V, relative to the detector, creating an electric field throughout the volume of the cell. The electric field drives positively charged particles onto the semiconductor detector.

The RAD7 uses the high electric field to attract the positively charged Polonium-218 daughter and then to count it. When the short-lived (it will reach the equilibrium with radon in about 15 min) polonium-218 nucleus decays, its alpha particle has a 50% probability of entering the detector and producing an electrical signal proportional in strength to the energy of the alpha particle. Subsequent decays of the same nucleus produce beta particles, which are not detected, or alpha particles of different energy. Different isotopes have different alpha energies, and produce different strength signals in the detector.

The RAD7 amplifies, filters, and sorts the signals according to their strength. The concentration is calculated automatically by the RAD7 in Bq m^{-3}. Humidity inside of chamber affect the sensitivity of the instrument, for this reason it is recommended to work with a relative humidity lower of 10%, in these conditions the detector has maximum efficiency and there is no humidity correction needed. RAD7 register the temperature and humidity inside the chamber during the measurement period. According to the manufacturer, with RAD7 is expected as much as one count every two hours (0.009 cpm) without any radon presence. This count rate, corresponding to an intrinsic background about 0.02 pCi l^{-1} (0.7 Bq m^{-3}). The RAD7 nominal sensitivity is 0.5 cpm pCi $^{-1}$ l (0.013 cpm Bq $^{-1}$ m^3) and the radon concentration range: 0.1 - 20000 pCi l^{-1} (4 - 750000 Bq m^{-3}).

2.1.3 Gamma spectrometry

Gamma spectrometry available in the physical laboratory of the Cosenza Department of the ARPACAL (Agenzia Regionale per la Protezione dell'Ambiente della Calabria) was used to perform measurements of radon concentration in

water and ^{226}Ra specific activity measurements for samples of Italian tuff.

Gamma spectrometry uses a Hyper Pure Germanium crystal detector (HPGe). A large electric field is applied across the Ge-crystal so that it is totally depleted. When a photon interacts in the depleted region of the crystal, electron-hole pairs are created. The number of produced charge pairs is proportional to the energy deposited by the photon. These pairs drift under an external electric field to the electrodes where they generate the pulse. The drift of charges produces an output pulse with an amplitude proportional to the energy deposited by the photon. Therefore, the greater the energy deposited in the detector, the greater the height of the pulse. Pulses are then amplified once more and sorted according to their size by a multichannel analyzer. The performance of a detector depends on its depletion depth, which is inversely proportional to the net impurity concentration in the detector material [41].

The experimental setup is composed by an Ortec HPGe detector (GMX), negatively biased, and integrated digital electronics. Its FWHM is of 1.94 keV, the peak-to-Compton ratio is 65:1 and the relative efficiency is 40% at 1.33MeV (^{60}Co). The detector is placed inside a lead shield to shield the background radiation environment.

2.1.4 Electrets

An electret is a dielectric material exhibiting a quasi permanent electrical charge. The charge of the electret produces a strong electrostatic field capable of collecting ions of opposite sign. E-PERM electrets (Teflon disk charged positively) were used to measure radon in water and radon exhalation rate from building materials in the IRL. An electret measures the ionization produced inside a chamber by the radon and its decay products. The quantification of the radon concentration is based on the correlation between the reduction of the surface voltage on the electret and the cumulative radon exposure in a passive chamber arrangement [42].

Chambers and the electret holders are made of electrically conducting plastic, low atomic number material, to minimize the response to the natural environmental γ radiation [42]. In the market there are two models of plastic chambers, model S and model L, each with a volume and construction design appropriate to short and long time interval measurements respectively (see Figure 2.1 left) . The model S chamber, presented in Figure (2.1 right), keeps

Figure 2.1: (Left) E-PERM system for radon gas measurement. (Right) Electret mounted on a chamber model S [43].

the electret covered and eliminate the unwanted background during storage or transport. The filtered inlet is necessary to allow radon into the chamber while excluding radon progeny or environmental ions. An annular filter over six small holes recessed in the top of the chamber serves this purpose. The air volume in the chamber is 210 ml. The model L (58 ml) can be used to make long term radon measurements or for shorter periods at higher radon concentrations measurements.

The electret surface potential voltmeter (see Figure (2.1 left)), called the electret voltage reader, it is an electronic instrument that reads out the electret voltage digitally in volts. In the same figure are shown the short-term chambers, the smaller long-term chamber and the Teflon electret.

The calculation of radon concentration can be obtained, as described in [44], from the variation of voltage during the exposition:

$$C_a = (\frac{V_i - V_f}{CF * t}) - BG \tag{2.1}$$

where C_a is the radon concentration in Bq m^{-3}, t is the exposure period in days, V_i and V_f the measured electret voltages before and after the exposition respectively, BG is the radon concentration equivalent of natural γ ray-radiation background and CF is the calibration factor in units of Bq m^{-3} d. For a given electret-chamber combination, CF is defined as a variation of the electret voltage per exposure at a concentration of 1 Bq m^{-3} d^{-1}. In [44]

is presented the study to calculate the calibration factor for the short-term and long-term systems. A series of experiments were conducted with known Rn concentration where electrets were exposed for known time periods, and the changes in their electrets voltages were measured. The calibration factor (CF) was calculated for each measurement using Eq. (2.1). Electrets are recommended for use between the voltages of about 750 V down to 200 V.

As described in [44], the overall random error of the E-PERM system consists of three parts: Error (E1) associated with the chamber volume, electret thicknesses, and other chamber parameters; Error (E2) associated with the reading of the electrets; Error (E3) associated with the uncertainty of the natural γ radiation background. Combining all the errors, the overall error (E) is given by:

$$E = \sqrt{\frac{Vi - V_f}{CF * T}(0.0025 + \frac{2}{V_i - V_f}) + (U\gamma * BG * D)^2} \tag{2.2}$$

where D is the conversion factor in Bq m^{-3} per μGy h^{-1} and $U\gamma$ is the gamma radiation uncertainty.

The lower limit of detection (LLD), defined as the radon concentration that can be measured within an error of 50%, depends mainly on the exposure period and the voltage region and whether it is a short or long-term E-PERM. Table 2.1 gives the range of lower limits of detection for various measurement periods [44]. Relative humidity has no effect on the performance of the electrets [44].

Period of measurement	**LT or ST electret**	**Range of LLD (Bq m^{-3})**
2	ST	20 to 28
7	ST	11 to 12
60	ST	8 to 9
30	LT	18 to 26
90	LT	10 to 11
365	LT	8 to 9

Table 2.1: Lower limits of detection for electrets[44].

The procedure for indoor measurements can be applied for measurements with water samples, the procedure is based on [45] with some modification as reported in Section (2.3.5), and for measurements with building materials

samples [46], as explained in the Section (2.2.3).

2.1.5 Radon closed chambers

The closed chamber in Plexiglas at IRL

The radon chamber in plexiglas, built in the Physical Department of Calabria University, is composed of 6 sheets of Plexiglas type G (Poly methyl methacrylate PMMA, plastic material colorless and clear, resistance to weathering and aging) with an area of 50 x 50 cm^2 and thickness of 1.0 cm. The choice of the material gives the opportunity to keep the instrumentation under control and allows a continuous visual inspection of the conditions of the experiment (about humidity on the walls, etc.). The closed chamber was sealed with screws and silicone for aquariums to ensure a good tightness and low air leakage through (in and out) the joints and through the walls, the last due to the fact that the insulating materials such as the plexiglas (dielectric constant of 3.6 at 50 Hz) have a very low radon permeability of 1.14 10^{-10} m^2 s^{-1} for 0.1 mm specimen thickness [14].

The gross volume of the chamber, 125 l, allow to minimize the radon back-diffusion effect, because the chamber net volume is more than 10 times larger than the volume of the samples studied [47]. The chamber is equipped with a removable lid for the insertion of the samples and the internal detector, a shelf for support instrumentation (meteorological stations, etc.), two tight connectors to allow the use of a detector outside the sealed chamber, a power supply for the internal detector and a 12 volt fan to homogenize the air inside the chamber, see Figure (2.2).

The closed chamber allows to measure the radon concentration inside the camera with an internal and external detector simultaneously, as shown in Figure (2.3) where the radon in air concentration as a function of time is presented. The empty black squares are RAD7 results obtained without humidity correction, the empty blue squares show the RAD7 results after humidity correction and the orange circles are measurements performed with a CPRD, is clearly visible the effect of humidity on RAD7 measurements. After correction, the measurements are well compatible.

Variations in laboratory temperature affect the temperature inside the chamber, in spite of the insulating properties of the Plexiglas (thermal conductivity of 0.19 W m^{-1} K^{-1}). The same behavior due to day/night effect

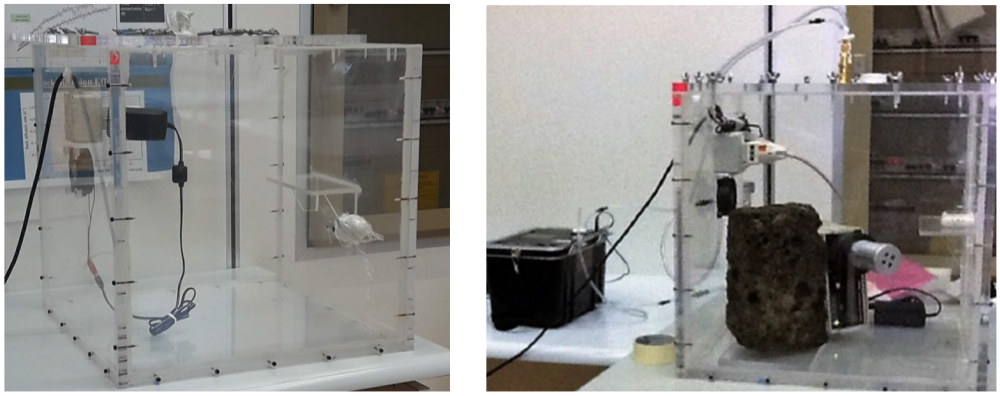

Figure 2.2: (Left) Radon chamber of the Physics Department of Calabria University. (Right) Radon exhalation rate experiment using internal (CPRD) and external (RAD7) detectors simultaneously [34].

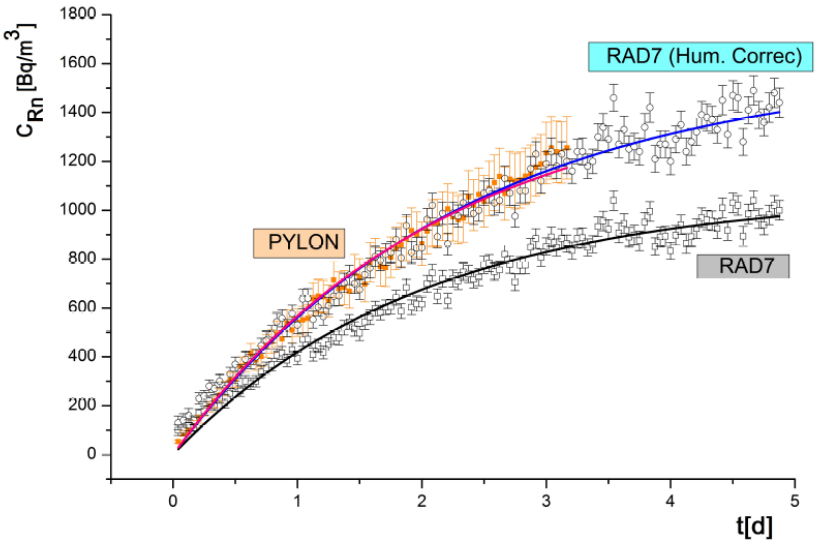

Figure 2.3: Radon activity concentration measurements inside the chamber using a CPRD (orange) and RAD7 (blue: humidity corrected data, black: no humidity corrected data) detectors [34].

there is inside and outside the chamber as shown in Figure (2.4), the mean value of the temperature inside the chamber is always 1-2 °C higher. This is probably related to the fact that the chamber is not completely sealed.

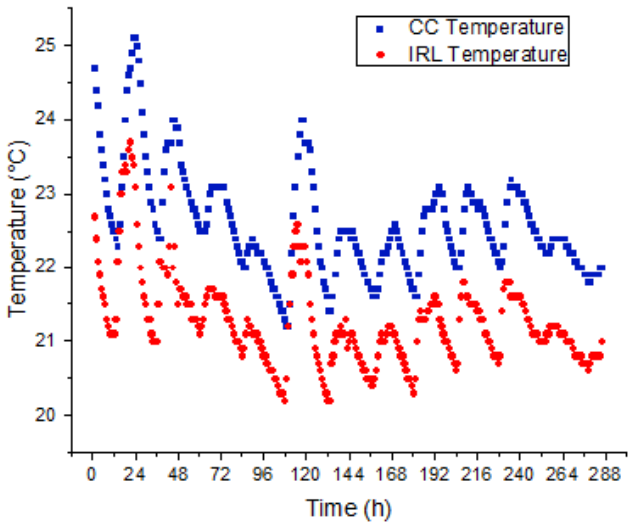

Figure 2.4: Temperature inside and outside (Ionizing Radiation laboratory) of the Plexiglas closed chamber.

In addition, in a wall of the chamber there is a gas-tight tap to introduce water samples in a container placed inside the hermetically sealed chamber. This feature allows to measure the radon concentration in water studying the rapidity of the spontaneous exhalation of the gas from the water. This original use of the chamber will be fully described in Section (2.3.6).

The closed chamber in tempered glass at NTL

The chamber in glass built in the Faculty of Science of the Escuela Superior Politécnica de Chimborazo, was made with six sheets of colorless glass (thermal conductivity of 0.6 - 1 W m^{-1} K^{-1}) of dimensions 50 x 50 cm^2 and thickness of 1.5 cm. The closed chamber was sealed with aquarium silicone and additionally they were fixed with aluminium angles on each edge. The gross volume of the chamber is 125 l.

The chamber is equipped with a removable lid for the insertion of the samples and the internal detector, a shelf for support instrumentation (meteorological stations, etc.), two tight connectors to allow the use of a detector outside the sealed chamber, a power supply for the internal detector use and a 12 volt fan to homogenize the air inside the chamber, see Figure (2.5 left), the figure on the right shows the chamber, interfaced with an external RAD7

Figure 2.5: (Left) Radon closed chamber at NTL.(Right) Radon exhalation rate experiment using an external RAD7 detector.

detector, during a measurement.

The closed glass chamber has a good thermal insulation, as can be seen in the Figure (2.6), while the temperature in the laboratory undergoes great variations, the temperature of the chamber remains quite constant. Day/night variations inside and outside the chamber are evident during the monitoring period.

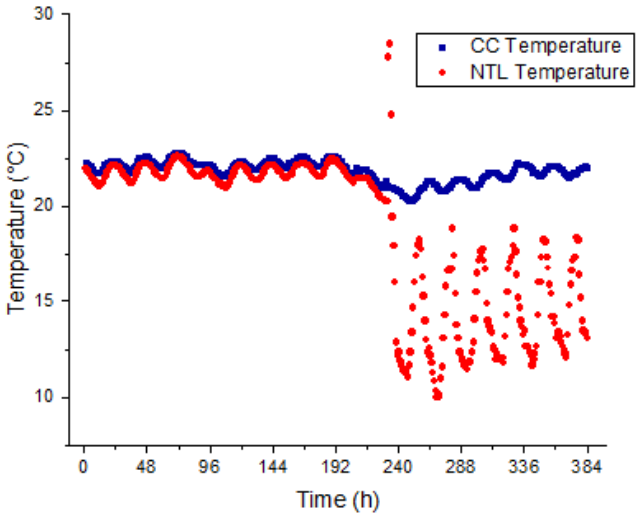

Figure 2.6: Temperature inside and outside (Nuclear Techniques laboratory) of the glass closed chamber.

In a wall of the chamber there is a gas-tight tap to introduce water samples in a container placed inside the hermetically sealed chamber. This feature allows to measure the radon concentration in water.

2.2 Radon exhalation rate measurement samples and techniques

2.2.1 Building material samples

The mass exhalation rate of many Italian samples largely used as building material has been extracted. The samples presented in this thesis are seven volcanic tuff samples and samples of sand from Calalunga di Montauro beach, phosphorite rocks, porphyry and a sample of pink granite from Sardegna. When it was necessary to reduce the moisture content of the samples, these were dried in a preheated oven.

Emphasis was placed on volcanic tuff coming from the Lazio Region and largely used in Italy [48]. The Lazio tuff is mainly the result of the action of the Sabatino Volcano in the period approximately between 600 000 and 300 000 years ago. In Roman times it was also used as a base to obtain hydraulic mortars. It has also been used for more recent constructions such as the foundation cities in the Pontine area. Old buildings and new buildings use this material because it is a rather resistant, light and workable rock but also for aesthetic reasons, see for example Figure (2.7) on the right. Figure (2.7 left), shows the variety of tuff samples from the Lazio region studied. The different color and texture of the samples is related to different chemical and physical properties of the samples. The weight of the samples in the figure varies from 1.6 to 6.2 kg.

Table 2.2 summarizes the characteristics of the samples of building material analyzed at IRL. A part of the samples of tuff Gray 1 and Gray 3 were crashed and transferred to a Marinelli beaker for gamma spectrometry analysis. The samples were weighed with a precision balance with a sensitivity of 1 g. For the crashed samples treated, the weight and the grain size, together with surface area and exposed crushed material thickness, are also reported in Table (2.2). All the samples have been used for tests with the close chamber except the samples in Table 2.2 marked with $*$, used for tests with the electrets technique.

In the NT laboratory were analyzed samples of brick, block, and concrete,

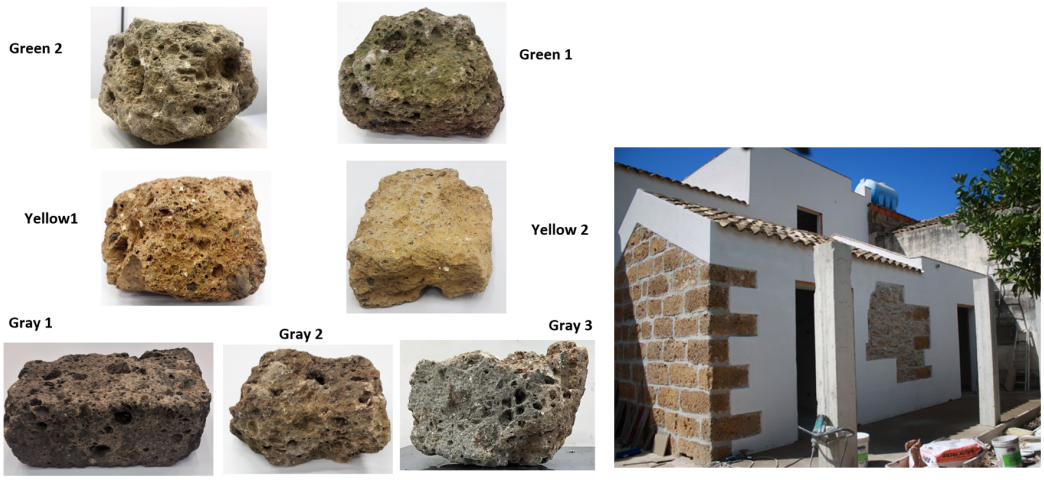

Figure 2.7: (Left) Samples of Lazio tuff with different colors, porosity, density, weight, volume and pumice stone inlays. (Right) Modern design of an Italian house, using volcanic tuff on the walls.

Name	**Weight kg**	**Exhalation area m^{-2}**	**Thickness cm**	**Grain size mm**	**Origin**
Gray 1 tuff	5.341				Lazio
Gray 2 tuff	6.115				Lazio
Gray 3 tuff	1.800				Lazio
Green 1 tuff	6.225				Lazio
Green 2 tuff	1.562				Lazio
Yellow 1 tuff	2.225				Lazio
Yellow 2 tuff	1.799				Lazio
Sand	1.610				Calalunga di Montauro
Phosphorite	0.742				Catanzaro
Porphyry	2.530				Catanzaro
Red granite	7.019				Sardegna
∗Yellow 3 tuff	0.114	0.013 ± 4%			Salerno
∗White granite	0.195	0.011 ± 2%			Salerno
Gray 1a tuff (crushed)	0.943	0.081 ± 1%	1.8±0.2	< 1	Lazio
Gray 1b tuff (crushed)	0.500	0.081 ± 1%	1.0±0.2	< 1	Lazio
∗Gray 1c tuff (crushed)	0.040	0.004 ± 2%	1.3±0.2	< 1	Lazio
Gray 3a tuff (crushed)	0.539	0.081 ± 1%	1.0±0.2	1 - 8	Lazio
∗Gray 3b tuff (crushed)	0.040	0.004 ± 2%	1.3±0.2	1 - 8	Lazio

Table 2.2: Characteristics of Italian building material samples.

materials widely used in foundations, floors and walls of houses and buildings in most provinces of Ecuador [49]. In addition, two types of granite, used for the construction of kitchen tops and bathroom furniture, a sample of pozzolan and decorative stone from the Chimborazo volcano were studied. Table (2.3) summarizes the characteristics of the samples of building mate-

rial analyzed in the NTL.

Name	Weight	Dimensions			Origin
		Length	Width	Thickness	
	kg	cm	cm	cm	
Concrete (home 1)	5.70	42.3 ± 0.1	26.7 ± 0.1	3.8 ± 0.1	Riobamba
Concrete (home 2)	5.20	42.1 ± 0.1	26.4 ± 0.1	3.8 ± 0.1	Riobamba
Granite A	4.60	56.3 ± 0.1	12.6 ± 0.1	2.7 ± 0.1	Riobamba
Granite B	5.90	56.3 ± 0.1	12.6 ± 0.1	2.7 ± 0.1	Riobamba
Block 1	5.20	57.0 ± 0.1	13.4 ± 0.1	3.2 ± 0.1	South Riobamba
Block 2	4.80	56.5 ± 0.1	13.4 ± 0.1	3.4 ± 0.1	North Riobamba
Brick 1	3.10	22.1 ± 0.1	8.1 ± 0.1	7.6 ± 0.1	Guano
Brick 2	3.30	22.2 ± 0.1	8.1 ± 0.1	7.7 ± 0.1	Guano
Brick 3	3.12	22.3 ± 0.1	8.0 ± 0.1	7.9 ± 0.1	Guano
Pozzolan	2.00				San Juan
Decorative stone	4.80	28.2 ± 0.1	9.2 ± 0.1	3.7 ± 0.1	San Andres

Table 2.3: Characteristics of Ecuadorian building material samples.

The brick is a solid ceramic material, it is a mixture of earth, sawdust (powdery particles of wood produced by sawing), ash and water. It is cooked at high temperatures in artisan ovens.

The block is a material composed of cement, powdered pumice stone and water, it is sun-dried in artisan factories. This material is very porous and it has a row four of perforations that reduce its weight and volume.

For the analysis of the concrete (mixture of cement, gravel and macadam) in the closed chamber, two compact rectangular blocks of were built, using the concrete of two houses under construction.

The two granite samples analyzed have different colors and tonalities but the same dimensions.

In the central part of the Figure (2.8) a typical construction made with brick and block is shown. The brick is used on the first floor for thick and strong walls, on the second and third floors the block is used. The placement of blocks and bricks to build the walls and floors is done manually using concrete in the joints. On the right of the Figure (2.8) the block and granite A and to the left the brick, concrete and granite B are shown.

2.2.2 Closed chamber technique

The closed chamber technique was used to determine the radon exhalation rate from building materials. The radon exhalation is due to the content of

Figure 2.8: Building materials typically used in Ecuador.

^{226}Ra as well as other properties of the material, such as porosity, permeability, emanation power, water content and surface coverage together with the environmental conditions in which it is located.

The experimental set-up consists on a closed chamber interfaced with an internal or external detector and has been described in the previous section.

Theoretical approach

To determine the exhalation rate, a sample is inserted into a chamber that will be hermetically sealed. The sample exhaling radon gas enriches the air in the chamber. Measuring the concentration of activity inside the chamber as a function of the time, an accumulation curve is observed after several days, depending on the properties of the sample, a condition of equilibrium is established. The mass balance of this process can be described with the following equation [50].

$$\frac{dC(t)}{dt} = \frac{E_o A}{V_{air}} + \lambda_l C_{bg} - \lambda_{Rn} C - \lambda_l C - \lambda_{bd} C \tag{2.3}$$

where λ_{Rn} is the radon decay constant, λ_l is the chamber leakage rate, λ_{bd} is the back diffusion rate, C_{bg} is the possible background due to the radon concentration in the laboratory, V_{air} is the net volume of air in the chamber, A is the area of the sample and E_o the initial radon exhalation rate of building material.

The first two terms on the right in Equation (2.3) indicate the contribution to the growth of chamber concentration due to the exhalation of the material and the entering of laboratory air in the chamber due to the chamber leakage; the last three terms show to decreasing concentration in the chamber due to respectively to the radon decay, the exit of the chamber air for leakage and the back diffusion effect [51].

Solving Equation (2.3) with the initial conditions t = 0, $C = C_i$, where C_i is the initial radon concentration inside chamber, we have the concentration evolution equation

$$C(t) = C_i e^{-\lambda_{eff} t} + \frac{E_o A}{V_{air} \lambda_{eff}} \left(1 - e^{-\lambda_{eff} t}\right) + \frac{\lambda_l C_{bg}}{\lambda_e ff} \left(1 - e^{-\lambda_{eff} t}\right) \quad (2.4)$$

where $\lambda_{eff} = \lambda_{Rn} + \lambda_l + \lambda_{bd}$

The chamber leakage constant, the radon background inside the chamber and radon back diffusion are in general necessary parameters for the radon exhalation extraction. In the case of this thesis, the contribution of back diffusion is negligible, both because the ratio between the volume of the samples and the chamber is below 10% and because the preferred measurement protocol is short-term as will be described later discussing the extraction technique of the exhalation coefficient.

Background measurements at IRL

In Italy the climate varies from the North to the South and from the costs to the high mountains. Temperatures are influenced by the Mediterranean sea and the Alps to the north of the country. There are four seasons, spring from March to May, summer from June to August, autumn from September to November and winter from December to February.

The Ionizing Radiation Laboratory is located in southern Italy, in Arcavacata di Rende, in the province of Cosenza, on the sixth floor of building 30 C in the Physics Department of the Calabria University. The building is

mainly made with concrete. It has a door and four windows and the laboratory air conditioning is realized with two hot/cold thermo-converter. The volume of the laboratory is 356 m^3. The IRL background has been monitored monthly for about a week using CPRD and electrets.

Table (2.4) shows the temperature and relative humidity inside the laboratory and IRL background measurements from January to November 2019. The minimum values correspond to the concentrations in summer (30 $\pm$ 5 Bq m^{-3}) while the maximum values in winter (51 $\pm$ 8 Bq m^{-3}) both measurements have been performed with a CPRD. The annual average radon concentration at IRL is 41 $\pm$ 1 Bq m^{-3}.

A similar seasonal pattern has been already discussed in scientific literature [52, 53], a parabolic fit to the data can be used to extrapolate the annual average concentration from measurements shorter to respect to a year.

Month	**Temperature indoor**	**Rel.humidity**	C_{Rn}	**Stand. desv.**	**Uncert.**	**Detector**
	^{o}C	**%**	**Bq m^{-3}**	**Bq m^{-3}**		
January	14	34	51	8	5	Lucas cell
February	20	40	46	9	5	Lucas cell
March	23	28	38	11	4	Lucas cell
April	22	44	43	12	4	Lucas cell
May	23	42	37	9	4	Lucas cell
June	23	52	34		6	Electret
July	22	53	30	5	3	Lucas cell
July	22	53	33		6	Electret
August	24	51	43	2	4	Lucas cell
September	27	47	39	11	4	Lucas cell
October	24	48	47		7	Electret
November	21	54	53		7	Electret
November	21	54	41	9	4	Electret

Table 2.4: Summary of indoor radon concentrations at IRL.

Figure (2.9) on the left, shows the radon concentration measurements (blue dots), made during the spring, and the temperature (pink dots), the measurement interval is one hour. The day/night effect is clearly visible, the radon concentration decreases while the temperature increases (during the day) and increases when the temperature decreases (during the night).

Inside the chamber fluctuations for day/night effect are modest, Figure (2.9) on the right shows the results of an experiment of radon concentration measurements, performed in 2019 May, inside the empty and sealed chamber. The background outside the chamber was monitored for 193 hours at an average temperature of 22 $\pm$ 0.5 ^{o}C and average relative humidity of 44 $\pm$ 3% .

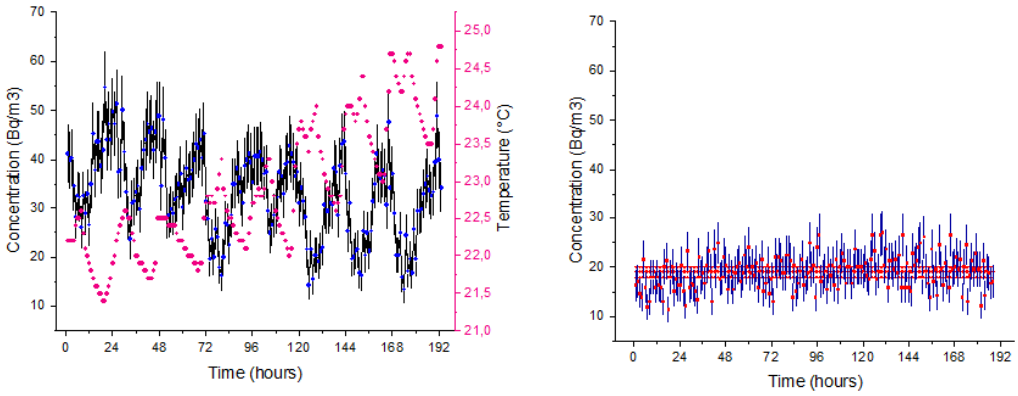

Figure 2.9: On the left, the Day/night effect on radon concentrations (blue dots) in the Ionizing Radiation laboratory is shown, in the same figure the laboratory temperature variation is also reported (pink dots). On the right is shown the radon concentration inside the empty and sealed chamber.

The background inside the chamber was monitored for 188 hours, at an average temperature of 23 ± 1.3 and average relative humidity of 42 ± 2%. The average radon concentration inside the chamber was 19 ± 1 Bq m^{-3}, depending on the closing instant, while in the laboratory was 33 ± 5 Bq m^{-3}. The fluctuations inside the chamber were about 80% less than outside the camera.

Background measurements at NTL

Ecuador has a tropical climate that varies with altitude and regions. The weather can varies widely on the same day. There are two seasons: Rainy (wrongly called winter) the weather is warm and rainy, lasts 4 to 5 months and runs from January to April or May. Dry season (wrongly called summer) that lasts 7 to 8 months and runs from May or June to December, it is the season with cool temperatures. However, Ecuador has very different microclimates depending on the four main regions that are: Costa, Sierra, Oriente y Galápagos.

The NTL is located in the sierra center, province of Chimborazo, Riobamba, in a single-floor building in the Faculty of Science of the ESPOCH University. The foundations are made of stone and concrete, brick walls and the concrete roof. It has two doors and 5 sealed small windows. It does not have heating or air conditioning. The volume of the laboratory is 179 m^3.

The background was monitored monthly, during my research in Ecuador, a weekend per month, in the period May - August 2018, using a RAD7 continuous monitor with measuring intervals of 60 minutes. The average concentration of the entire period was 28 ± 6 Bq m^{-3}, the average laboratory temperature was 22 ± 0.3 ^{o}C.

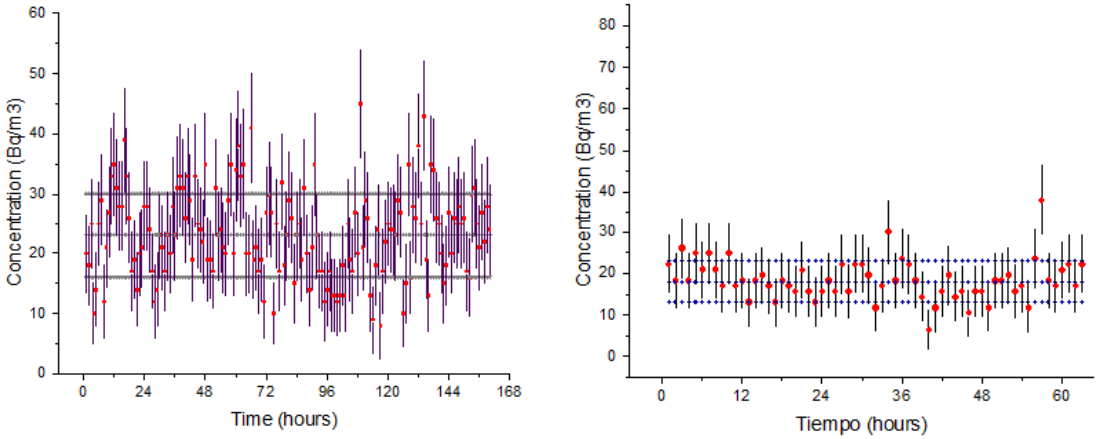

Figure 2.10: On the left, a NTL laboratory radon activity concentration measurement. On the right, the results of a monitoring of the radon concentration inside the empty and sealed chamber.

Figure 2.10 (left) shows a single 7-days measurement at NTL. Also in this case a day/night effect is visible. Figure (2.10) (right) shows the results of radon concentration measurements inside the empty and sealed chamber, performed in the dry season (July). The background outside the chamber was monitored for 161 hours at an average temperature of 21.5 ± 0.3 ^{o}C. The background inside the chamber was monitored for 63 hours, at an average temperature of 22.5 ± 0.3 ^{o}C and average relative humidity of 19 ± 1%. The average radon concentration inside the chamber was 18 ± 5 Bq m^{-3}, while in the laboratory was 23 ± 7 Bq m^{-3}. The average radon concentration inside the chamber was less than the average concentration in the laboratory and the fluctuations are smaller.

Chamber leakage calculation

The leakage is a fundamental parameter to characterize the chamber. To calculate the leakage of the chamber it is necessary to enrich the chamber with radon gas, for example by closing a high-exhaling material or using a

source inside the chamber, then the enriched chamber with a concentration C_i, containing only the detector can be sealed. Inside the chamber, the concentration decreases both due to the spontaneous decay and for the leakage of the chamber. The measurement for several days of the concentration can be used to calculate the leakage.

Starting from Equation (2.3), the concentration decreasing inside the empty chamber is described by the following equation:

$$\frac{dC}{dt} = -\lambda_{Rn}C + \lambda_l C_{bg} - \lambda_l C \tag{2.5}$$

The first term on the right indicates the spontaneous radon decay, the second and third terms represent the exchange of laboratory and chamber radon due to the chamber leakage.

Resolving Equation (2.5), with the initial conditions t = 0, $C = C_i$, we have

$$C(t) = C_i e^{-\lambda_{eff}t} + \frac{\lambda_l}{\lambda_{eff}}C_{bg} - \frac{\lambda_l}{\lambda_{eff}}C_{bg}e^{-\lambda_{eff}t} \tag{2.6}$$

where $\lambda_{eff} = \lambda_{Rn} + \lambda_l$

Fitting the experimental data with the function (2.6) with λ_{eff} and C_i free parameters and C_{bg} fixed, is possible to calculate the leakage rate by subtracting $\lambda_l = \lambda_{eff} - \lambda_{Rn}$ where $\lambda_{Rn} = 2.09838(44)\ 10^{-6}s^{-1}$ [54].

A second method, widely used in scientific literature (see for example [50]), uses only the first few data. Assuming a linear decreasing in the early hours, this method calculates the leakage rate by comparing the experimental slope with the expected (theoretical) slope if only spontaneous decay occurs.

In the theoretical case the chamber has zero leakage and the concentration decreases with the decay law.

$$C_{th} = C_i e^{-\lambda_{Rn}t} \tag{2.7}$$

and, for $t \to 0$, the slope

$$m_{th} = \frac{d}{dt}C_{th} = -\lambda_{Rn}C_i \tag{2.8}$$

In the experimental case

$$m_{exp} = \frac{dC}{dt} = -\lambda_{eff} C_i + \lambda_l C_{bg} \tag{2.9}$$

therefore, comparing the slopes in the Equation (2.8) and Equation (2.9)

$$m_{th} - m_{exp} = \lambda_l (C_i - C_{bg}) \tag{2.10}$$

the leakage rate can be determined

$$\lambda_l = \frac{m_{th} - m_{exp}}{C_i - C_{bg}} \tag{2.11}$$

The experimental slope m_{exp} and C_i can be extracted applying a linear fit to the measurements of the first hours.

For the measurements presented in this thesis we use the first 24 hours data collected with a time interval of one hour and an empty chamber enriched with gas radon corresponding to an initial concentration greater close to 1000 Bq.

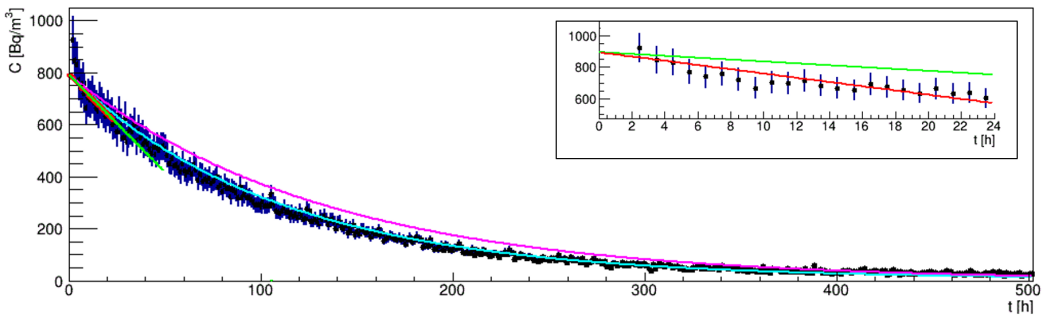

Figure 2.11: Radon concentration decreasing curve measured inside the sealed radon chamber. The light blue curve is the result of the global fit and the pink is the theoretical curve expected. The insert shows the initial set of data. The red line is the result of the linear fit and the green line indicates the theoretical expectation.

Figure (2.11) shows the typical decreasing behavior in a leakage measurement. The curves shows the decay fit result according with Equation (2.6) assuming no leakage (pink line) and the curve result of the fit (light blue) obtained. In the insert, the slopes of the red (experimental) and green (theoretical) fit are shown.

Evaluation of the radon exhalation rate

The chamber concentration growth is described by Equation (2.4), the initial radon activity concentration inside the chamber is due to only the background. After an accumulation of several days, the radon concentration in the chamber will approach an equilibrium value, given by the equation:

$$C(\infty) \cong \frac{E_o A}{V_{air}\lambda_{eff}} + \frac{\lambda_l C_{bg}}{\lambda_{eff}} \tag{2.12}$$

or

$$E_o = (C_\infty \lambda_{eff} - \lambda_l Cbg)\frac{V_{air}}{A} \tag{2.13}$$

where E_o is the surface exhalation rate. The parameters C_∞ and λ_{eff} are extracted fitting the intere data sample with the function (2.6).

In the case of samples with irregular shape, it is not simple to determine the exhalation surface without introducing a large uncertainties, in this case the area A can be replaced with the mass m of the sample and the mass exhalation rate is calculated with:

$$E_o = (C_\infty \lambda_{eff} - \lambda_l C_{bg})\frac{V_{air}}{m} \tag{2.14}$$

A different method for calculating the exhalation rate is by studying the rapidity of increasing of the concentration differentiating the equation (2.4) that, for t$\rightarrow$0 is:

$$\frac{dC}{dt} = m_g = \frac{E_o A}{V_{air}} + \lambda_l C_{bg} - \lambda_{eff} C_i \tag{2.15}$$

or

$$E_o = (m_g - \lambda_l C_{bg} + \lambda_{eff} C_i)\frac{V_{air}}{A} \tag{2.16}$$

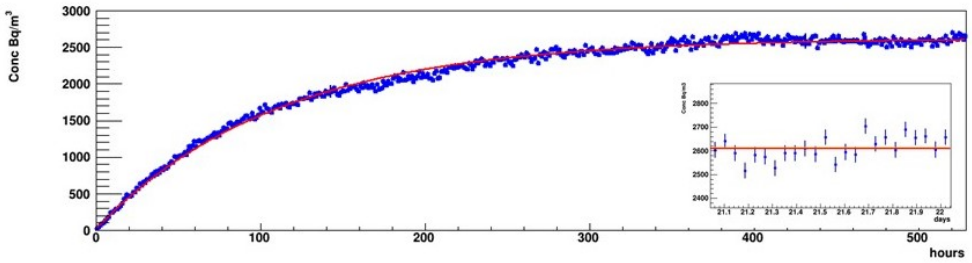

Figure 2.12: (Top) Activity concentration as function of time, of sample Green 2. (Bottom) Linear and constant fit performed to the last 24 hours data.

where m_g represents the rapidity of accumulation of radon gas inside the chamber, which is directly related to the radon exhalation rate from the material.

The mass exhalation rate E_o will be:

$$E_o = (m_g - \lambda_l C_{bg} + \lambda_{eff} C_i)\frac{V_{air}}{m} \tag{2.17}$$

where the initial slope m_g can be extract from a linear fit.

Finally the surface exhalation rate or mass exhalation rate can be calculated by Equations (2.16) and (2.17) respectively.

Figure (2.12 top) shows, for example, the studies performed with the sample Green 2. The red curve is the result of the global fit and the blue dots are the experimental data. The same Figure (2.12 bottom) shows also the result of linear and constant fit to the last 24 hours data accumulated, performed to evaluate the equilibrium reached in the chamber.

Figure (2.13) on the left shows the radon accumulation curve inside the sealed chamber. On the right the initial part of the growth is emphasized.

2.2.3 Electrets technique

The electrets technique can be used as an alternative to the closed chamber technique. The experimental setup consists of a small chamber having an

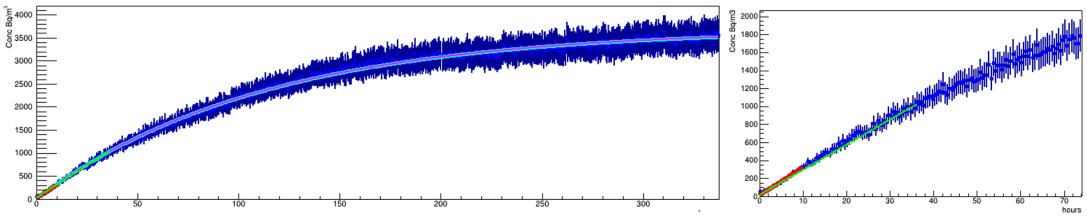

Figure 2.13: (Left) Radon accumulation curve inside the closed chamber. The blue curve is the result of the global fit. (Right) Initial accumulation phase, the green line is the result of the linear fit and the red is the theoretical line.

electret at the bottom and a filtered inlet at the top. Radon gas entering the chamber and the decay products formed inside the chamber generate ions in the air that are collected by the electret.

Radon exhalation rate calculation procedure

This technique uses a four liters jar with rubber seals as radon leak tight accumulator and a detection system chamber-electret. Figure (2.14) shows an example of experiment.

The procedure consists of enclosing the sample of material held by small adhesive at the bottom of the the glass jar and sealing it tightly with the detection system suspended in the air. At the end of the desired exposure period the radon concentration in air is calculated. Similar arrangement without a sample allow to obtain the background radon concentration. The net radon concentration is obtained by subtracting the background concentration from the concentration measured with the sample.

$C_{Rn_{av}}$, the integrated average radon concentration in Bq m^{-3}, is given by the equation [46]:

$$C_{Rn_{av}} = \frac{E_o A}{V \lambda_{Rn}} \{1 - [\frac{1}{\lambda_{Rn} T}(1 - e^{-\lambda_{Rn} T})]\} \tag{2.18}$$

where E_o is the surface radon exhalation rate Bq m^{-2} d^{-1}, A is the area in m^2, λ_{Rn} is the decay constant of radon in d^{-1}, T is the accumulation time in days and V is the air volume of the accumulator in m^3.

The surface exhalation rate can be extracted as

Figure 2.14: Radon exhalation measurement using the electret ion chambers technique.

$$E_o = \frac{C_{Rn_{av}} V \lambda_{Rn}}{KA} \tag{2.19}$$

where K is the constant inside the braces sign in (2.18) and C_{Rn} in the jar is obtained with the procedure described in Section (2.1.4).

The mass exhalation rate E_o (Bq kg d^{-1}) is given by the Equation (2.20):

$$E_o = \frac{C_{Rnav} V \lambda_{Rn}}{Km} \tag{2.20}$$

where m is the sample mass in kg.

2.3 Radon in water measurement samples and techniques

2.3.1 Study areas

Calabria region

The region is generally known as the toe of the boot of Italy and is a long and narrow peninsula which stretches from north to south for 248 km, with a maximum width of 110 km. Some 42% of Calabria's area is mountainous, 49% is hilly, while plains occupy only 9% of the region's territory. It is surrounded by the Ionian and Tyrrhenian seas.

In central-northern Calabria, soil-gas radon concentrations are affected by the main geological fault systems: the main pathways of exhalation, in fact, correspond to the regional WNW-ESE shearing zones, the E-W fault system in the Rossanese study area, the N-S system in the Crati Graben and the Catanzaro Trough, and the NE-SW system in the Catanzaro Trough. Greatest concentrations are generally to be found along recent tectonic structures, mostly at the margins of the Sila Massif; in addition, radon concentrations generally increase with decreasing distance from the faults, for further details [55] where a study about the correlation between soil radon concentration and faults in the Northern Calabria is reported.

The climate is generally of Mediterranean type, with the ionic coastline drier and arid than the Tyrrhenian one. Temperatures generally along the coast never drop below 10°C and never rise above 40°C, but in inland areas in the summer months it can have peaks of 42-44 °C. On the Apennines and inland areas, from Pollino, Sila to Aspromonte, the climate is cold continental with cold and snowy winters. Summer is mild and thunderstorms are not lacking.

The monitored springs in Calabria are public water sources. The selection of the springs was made taking as a guide the list prepared by the Minister of Public Works of Italy in 1941 [56] and those suggested by the inhabitants of different towns of the Calabria region or recent geological maps. Special emphasis was placed on a spring located in the municipality of Castiglione Cosentino, in the northern region of Calabria, the Orbo spring. This geographical area has a high concentration of radon in the soil [55] and it is characterized by a very high historical seismicity. In particular, Orbo spring has been extensively studied since 2011.

Province of Chimborazo

The province of Chimborazo is one of the 24 provinces of the Republic of Ecuador, located in the south central part of the country, in the geographical area known as the interandina region or sierra. Its capital is the city of Riobamba. It occupies a territory of about 5287 km ^{2}, being the seventeenth province of the country by extension.

The Province of Chimborazo has several reliefs: **Relief of Cordillera**, which corresponds to 78% of the territory, the Eastern and Western Cordillera crosses the Province; **Serrania** with an area corresponding to 14% of the provincial surface, this relief is located in the central part of the province in the cities of Guano, Colta, Riobamba, Guamote, Alausí and Chunchi; **Glacier Valley** with an area of 5% of the surface, this relief is located in the Collanes Valley, Cubillines Valley and the area between Chimborazo and Carihuairazo; **Tectonic Valley**, corresponds to 2% of the surface, this relief corresponds to the geological faults of Pallatanga, Chambo and Chanchán; **Piedemonte** corresponds to 1% of the surface, this type of relief can be found in the cities of Alausí, Pallatanga and Cumandá [57]
.

The province presents internal geodynamic processes, a high volcanism due to the volcanic activity of Tungurahua as permanent threats to the population and road infrastructure. The permanent seismicity throughout the provincial territory is due to geological faults, its irregular relief and steep slopes, which gives rise to external geodynamic processes such as mass movements, subsidence and expansiveness throughout the provincial territory.

Chimborazo is characterized by presenting a climatic heterogeneity, so over 4.600 m.a.s.l. it is glacial, between 3.000 and 4.000 m.a.s.l. it is paramo. Going down to 2.000 m.a.s.l. we found a dry mesothermic climate, in the areas near the coast a humid and semi-humid mesothermic type climate predominates. The average temperature is 13 °C.

Information on radon concentration in the soil of the province of Chimborazo is not available in the scientific literature.

In the province of Chimborazo, wells and springs that constitute the drinking water supply of the cities of Riobamba and Guano and the community of Calera-Shobol Pamba, San Juan were monitored. In addition, the wells that supply water to two universities of the city of Riobamba (ESPOCH, UNACH) and other springs open to the public located in different towns were analyzed.

The selection of wells and springs was carried out based on the hydrogeological guide of Ecuador [58], published by the National Institute of Metereology and Hydrology (INAMHI), which details the aquifer system of the Chimborazo - Altar Hydrogeological Unit.

2.3.2 Sampling protocol

Our sampling protocol is based on ISO 13164-3: 2013 standards, to which have been added some recommendations supported by experience and by the particular detector to obtain reliable and comparable results and to guarantee the repeatability of the measurement. The elements of the sampling protocol are detailed below:

a) Spring or well information
This item includes the identification and registration of the geological characteristics of the place where the water source is located, the structural characteristics of the spring, the geographical coordinates, age of the fountain, air temperature, water temperature and water flux and all the general information available.

b) Containers and caps used for sampling
The water collection containers must have the volume required by the measurement method. The containers and caps can be the standard supplied by the company or by others that guarantee low radon permeability and high tightness. Dense plastic or glass containers and caps with an internal Teflon, rubber or plastic disc are recommended. The bottles must be previously washed and dried.

c) Water sampling
At the time of sampling, the bottle is positioned as close as possible to the water outlet and the inclined position, allowing the flow of water to flow along the walls of the container. The bottle must be filled up to the overflow and then closed under the flow of water. If the source or the well is equipped with a tap, it is necessary to let the water flow for a few minutes or in any case until the water temperature reaches a stable value, after which the tap must be regulated until a continuous flow is obtained with minimal turbulence. The sample is considered adequate if there are no air bubbles in the bottle. The caps must be sealed with plastic tape to avoid leaks.

An alternative procedure is to fill without turbulence a larger container, and then immerse the sample bottle under water, in the lowest position of the container and screw the cap.

d) Number of samples and spring sampling frequency
It is necessary to collect at least three water samples to take into account the variability of the measurements (due to the operator's ability or the supply

characteristics of the source). All water samples should be taken in a short period of time and under the same sampling conditions. It is suggested to monitor the springs twice a year, during the dry and rainy season.

e) Sample label
Samples must be labeled and a unique code assigned.

f) Transport of samples
Properly packed bottles must be transported upside down in a thermal bag. In the laboratory, samples should be kept in the refrigerator until measured. The time between sampling and analysis must not exceed a few hours.

2.3.3 Emanometric technique

The emanometric technique allows an indirect measurement of the concentration of radon activity in the water, thanks to the emanation of the radon dissolved in the water sample in the air by degassing. Degassing can be carried out by immersing a porous stone in the liquid and blowing air into it. The numerous bubbles produced will favor the migration of radon in water to air bubbles. These, collected, dehumidified and inserted in a detector, will allow measurement in the air.

The experimental set up consists of a detector and a degassing system, and a pump to circulate the air through the porous stone, which form a closed circuit.

In particular, the **IRL set up** consists of the Lucas cell interfaced with the Pylon AB-5 Portable Radiation Monitor and Mi.am H2O radon kit, see Figure (2.15). The apparatus requires a degassing period of 5 minutes, that is realized using the AB-5 internal pump. When it is completed, the counting of the radon decays in the Lucas cell is activated for five intervals, with time intervals of one minute. The extraction efficiency, according to the manufacturer, is close to 100% . The Figure (2.15) shows the configuration, in particular, the blue porous stone inside the bottle, the dehumidification filter, the fluximeter.

The radon concentration in the water sample is given by the following equation [59]:

$$C_w = \frac{(cpm - bg) * CF * e^{\lambda \Delta t}}{S * 100} \tag{2.21}$$

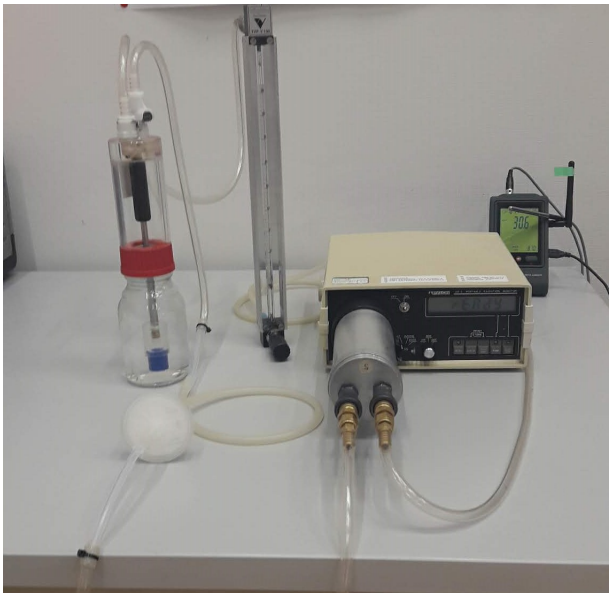

Figure 2.15: Water measurement with the emanometric technique at IRL. The blue porous stone in the bottle.

where *cpm* is the number of counts per minute, obtained in the 5 minutes of the counting phase, *bg* is the number of counts per minute of Lucas cell background, S is the cell sensitivity expressed in cpm Bq^{-1} m^{-3}, CF is system calibration factor that take into account the counting far from the secular equilibrium and $e^{\lambda \Delta t}$ is the correction factor for the elapsed time from sampling to counting, needed if the measurement is not performed immediately after sampling.

The **NTL set up** consists of the RAD7 continuous monitor and Durridge RAD H2O Rn kit. Figure (2.16) shows the set up used at NTL. When the degassing period has been completed (5 minutes), the system will wait a further five minutes. It will then start counting, after five minutes, it will print out a report. The same thing will happen again five minutes later, and for two more five-minute periods after that. At the end of the run (30 minutes after the start), the RAD7 prints out a summary, showing the average radon reading from the four cycles counted, a bar chart of the four readings, and a cumulative spectrum. The extraction efficiency is the 99% for a 40 ml sample and 94% for a 250 ml sample.

Figure 2.16: NTL emanometric apparatus: RAD7 monitor and Durridge RAD H2O Rn kit.

2.3.4 Gamma spectrometry technique

Radon activity concentration in water is based on the detection and quantification of gamma radiation, emitted by the short-lived daughters of the radon (^{214}Bi and ^{214}Pb) in the sample. The formula used is:

$$C_{Rn} = \frac{C_{Bi214}/\sigma^2{}_{C_{Bi214}} + C_{Pb214}/\sigma^2{}_{C_{Pb214}}}{1/\sigma^2{}_{C_{Bi214}} + 1/\sigma^2{}_{C_{Pb214}}} \tag{2.22}$$

Where C_{Rn} is the radon activity concentration, C_{Bi214} is the activity concentration of ^{214}Bi and C_{Pb214} is the activity concentration of ^{214}Pb.

The uncertainty is given by:

$$\sigma_{Rn} = \frac{1}{\sqrt{1/\sigma^2{}_{C_{Bi214}} + 1/\sigma^2{}_{C_{Pb214}}}} \tag{2.23}$$

This technique requires the collection of the spring water sample directly in a 1 liter Marinelli beaker, then properly sealed to prevent the spread of radon gas. Before the start of the measurement, it is necessary to wait three hours, the time necessary to reach the secular equilibrium between radon and

its short-lasting *gamma* emitting daughters.

Samples were counted for 251799 seconds and the spectra were analyzed to obtain the activity concentration of ^{214}Pb and ^{214}Bi. The 295.21 keV and 351.92 keV ^{214}Pb and 1120.29 keV ^{214}Bi gamma ray lines were used to determine the ^{222}Rn activity concentration.

Efficiency and energy calibrations were performed using a multi-peak Marinelli geometry gamma source with 1 l capacity, covering the energy range 59.54–1836 keV, customized to reproduce the exact geometries of samples in a water-equivalent epoxy resin matrix.

The Gamma Vision (Ortec) software was used for data acquisition and analysis.

The massic activity of each identified radionuclide was calculated using the following formula:

$$C = \frac{N_E}{\epsilon_E t \gamma_d M} \tag{2.24}$$

where N_E indicates the net area of a peak at energy E, ϵ_E and γ_d are the efficiency and yield of the photopeak at energy E, respectively, M is the mass of the sample (kg) and t is the live time (s).

The calculated value was corrected for the internal absorption by using the mass attenuation coefficients reported in the literature. The measurement uncertainty is a combined standard one at coverage factor k = 2, taking into account the following components: uncertainty counting statistics, uncertainty in nuclear data library, uncertainty due to calibration efficiency, uncertainty about the quantity of the sample, uncertainty due to the correction for self-absorption.

The Figure (2.17) shows the instruments of the ARPACAL of Cosenza and a Marinelli glass.

2.3.5 Electret technique

A water sample is placed on the bottom of a glass container. A chamber-electret system is inserted into the container and suspended under the lid.

Figure 2.17: (Left) ARPACAL gamma spectrometer. (Right) Marinelli beaker.

The container is tightly closed and shaken. The radon dissolved in the water spreads in the air. After the exposure period, the electret is analyzed and the radon concentration in the water is calculated.

The set up consists of an E-PERM-S chamber, a short term electret mounted at the base of the chamber, a four liter jar and a 136 ml bottle with the sample inside.

The procedure, in particular, is as follows: immediately before the start of the measurement, the voltage of the electret is recorded. The open chamber is hung under the cap of a jar. The large glass jar is then placed horizontally on a table and the cap of the sample bottle must be unscrewed gently inside the jar, see Figure (2.18 left). At this point it is possible to screw the cap of the can and carefully bring the jar upright allowing the water in the sampling bottle to pour onto the bottom, see Figure (2.18 right). It is necessary to quickly tighten the jar cap to avoid radon leakage, install the rubber sealing collar, cover the jar with plastic film and record the date and time of the start of the test. After the exposure period (1-2 days, depending on the concentration) the jar is opened and the final voltage measured and recorded.

The radon concentration in water is given by the following equation:

$$C_w = (C_a\ C_1\ C_2)/2 \tag{2.25}$$

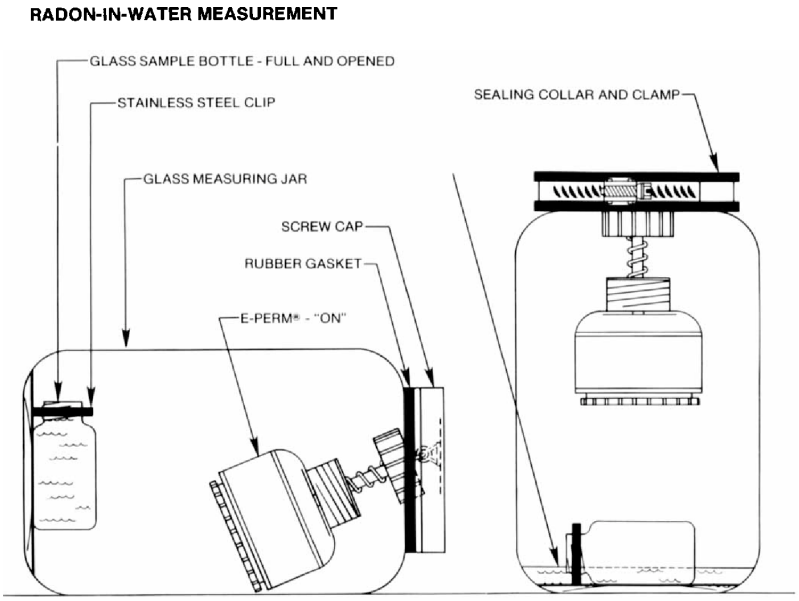

Figure 2.18: Radon in water measurement procedure with electret technique [60].

where C_a is the radon concentration in air, C_1 and C_2 are constants, defined as follows.

$$C_1 = e^{\lambda_{Rn} TD} \qquad C_2 = \frac{55.55\ \lambda_{Rn}\ TA}{1 - e^{\lambda_{Rn} TA}}$$

where, TD is the interval from the time of collection of the water sample to the time of inserting the sample bottle into the jar for analysis, expressed in days; TA is the interval from the time the sample bottle was inserted into the measurement jar until the chamber was removed from the jar, expressed in days and λ_{Rn} is the decay constant of radon in day^{-1}.

The manufacturer recommends to multiply the result by the calibration correction of 1.15 to get the final radon in water concentration (tests USEPA)[60].

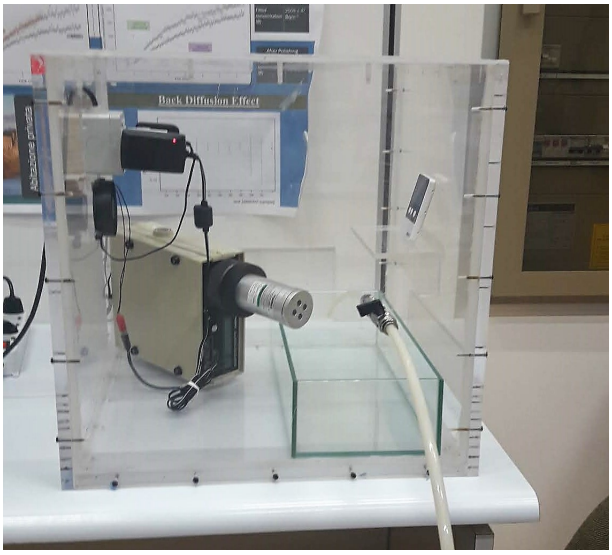

Figure 2.19: Experimental set-up for measuring radon concentration in water sample in a closed chamber.

2.3.6 Closed chamber technique

The experimental set-up is composed of the closed chamber of 125 l, already described before, with inside a container in glass with a capacity of 5 liters, interfaced with an internal and/or external detector (Figure (2.19)). A system of tubes that connect the exterior and interior of the chamber, ensure low turbulence during the process of entering the water into the container.

The procedure consists in placing a known volume of water inside the tight chamber through the tap (see Figure (2.19)) and measuring the growth of the radon activity concentration in the air inside the chamber.

This is an original technique tested for the first time at IRL. The spontaneous emanation of the gas from the water when interfaced with the air, already adopted with electret techniques, is now exploited with the closed chamber. The main advantages are related to the possibility to perform research, the chamber is an instrument in which environmental parameters, such as temperature and humidity, and other parameters, can be kept under control and measurements of water/air transfer coefficient and measurements of the transfer velocity can be studied as a function of these parameters.

This method can be explained as follows. If the physical problem is reduced to a one-dimensional diffusion, the Equations (2.26) and (2.27) cor-

responding respectively to the water and air sections respectively [61].

$$\frac{\partial C_w}{\partial t} = D_w \frac{\partial^2 C_w}{\partial z^2} - \lambda_{Rn} C_w \tag{2.26}$$

$$\frac{\partial C_a}{\partial t} = D_a \frac{\partial^2 C_a}{\partial z^2} - \lambda_{Rn} C_a \tag{2.27}$$

where C_w is the radon activity concentration in water, C_a is the radon activity concentration in air, D_w is the diffusion coefficient of radon in water and D_a is the diffusion coefficient of radon in air.

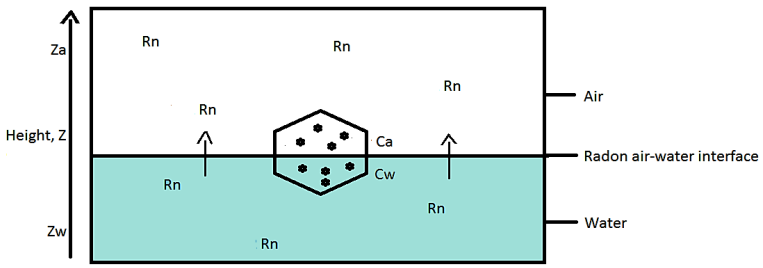

Figure 2.20: One-dimensional scheme of the radon transfer from the water to the air volume in the glass container and the chamber.

At the water-air interface, the diffusion is driven by the concentration gradient and can be expressed as:

$$F(t) = k[C_w(t) - \alpha C_a(t)] \tag{2.28}$$

where F is the flux of radon from water to air (Bq m^{-2} s^{-1}), k is the radon transfer velocity coefficient (m s^{-1}) and α is the Ostwald coefficient $\alpha = C^w_{eq}/C^a_{eq}$ which describes the ratio of the radon concentration in water at the equilibrium state (C^w_{eq}) to the radon concentration in air at equilibrium state (C^a_{eq}).

The Ostwald coefficient depends on temperature and salinity [62]. The Ostwald coefficient according the mathematical formula given by Weigel (1978); $\alpha = 0.105 + 0.405e^{-0.0502T}$ where T is the temperature in degrees

Celsius.

At the time that radon is not diffusing from the water to the air, it has the equilibrium condition. The change in the concentration of radon gas activity in the air inside the chamber is given by:

$$\frac{\partial A_a(t)}{\partial t} = SF(t) - \lambda_{Rn} A_a(t) \tag{2.29}$$

where S is the water-air interface area. The first term on the right is the addition of radon in the time interval Δ t due to the flux across the interface and the second term is the loss due to radon decay in the air.

Dividing Equation (2.29) by the volume of the air:

$$\Delta C_a(t) = \frac{SF(t)\Delta t}{V_a} - \lambda_{Rn} C_a(t)\Delta t \tag{2.30}$$

Combining Equations (2.28) and (2.29), result in an equation which governs radon concentration in air:

$$\Delta C_a(t) = \frac{S[k(C_w(t) - \alpha C_a(t))]\Delta t}{V_a} - \lambda_{Rn} C_a(t)\Delta t \tag{2.31}$$

Similarly, the radon activity concentration for radon atoms diffusing and decaying from water can be expressed as:

$$\Delta C_w(t) = -\frac{S[k(C_w(t) - \alpha C_a(t))]\Delta t}{V_w} - \lambda_{Rn} C_w(t)\Delta t \tag{2.32}$$

where V_w is the volume of the water. The negative sign in Equation (2.32) indicates the radon atoms are diffusing from the water when the concentration in the water is higher than in the air.

Equations (2.31) and (2.32) form two coupled first order differential equations that cannot in general be solved analytically. However, the equations can be expanded and written as finite difference equations and then solved using a numerical procedure:

$$C_a(t_i) = C_a(t_i - 1) + \frac{S[k(C_w - \alpha C_a)]}{V_a}(t_i - t_i - 1) - \lambda_{Rn} C_a(t_i - t_i - 1) \tag{2.33}$$

Similarly, the expanded equation for radon concentration in water is:

$$C_w(t_i) = C_w(t_i-1)+\frac{S[k(C_w-\alpha C_a)]}{V_w}(t_i-t_i-1)-\lambda_{Rn}C_w(t_i-t_i-1) \quad (2.34)$$

where $C_a(t_i-1)$ and $C_w(t_i-1)$ are the initial radon concentration in air and water at the initial time (t_i-1) respectively. $C_a(t_i)$ and $C_w(t_i)$ are the iterated radon concentration in air and water at the step time (t_i), respectively.

On the other hand, the initial radon concentration in the water can be estimated by using the experimental concentration value in air at equilibrium (C_a^{eq}) to obtain the total activity at the initial time (A_o) by correcting for the decay.

$$A_o = (C_a^{eq}V_a + C_w^{eq}V_w)e^{\lambda_{Rn}t_{eq}} = C_a^{eq}V_a + \alpha C_a^{eq}V_w)e^{\lambda_{Rn}t_{eq}} \quad (2.35)$$

$$\frac{A_o}{V_w} = C_w = (C_a^{eq}\frac{V_a}{V_w} + \alpha C_a^{eq})e^{\lambda_{eff}t_{eq}} \quad (2.36)$$

$$\lambda_{eff} = \lambda_{Rn} + \lambda_l$$

where t_{eq} is the time when the equilibrium state is achieved and λ_l is the chamber leakage. Taking into account that initially there is a background radon concentration in the air volume of the chamber, the equation can be written as:

$$C_w = (C_a^{eq*}\frac{V_a}{V_w} + \alpha C_a^{eq*})e^{\lambda_{eff}t_{eq}} \quad (2.37)$$

Where C_a^{eq*} is the difference between the radon activity concentration in air at equilibrium state and chamber background.

In order to exemplify this technique, Figure (2.21) shows the radon concentration in air inside the chamber in a complete experiment, using a water sample of 4 liter from San Giovanni in Fiore, spring located in the region of Calabria-Italy. The first 16 hours was used to assess the background radon concentration inside the chamber, before entering the water and due to the laboratory concentration, see Figure (2.21) section A, the observed value was

21 ± 3 Bq m^{-3}. The accumulation curve, Figure (2.21) section B, is used to calculate radon activity concentration in air (2927 Bq m^{-3}) and the time at equilibrium state (40 hours). Extending the measurement, is possible to study the decay curve, Figure (2.21) section C and evaluate the chamber leakage during the experiment. The leakage was extracted from the global fit, detailed in the Section (2.2.2), the result was 0.0012 ± 8% h^{-1}.

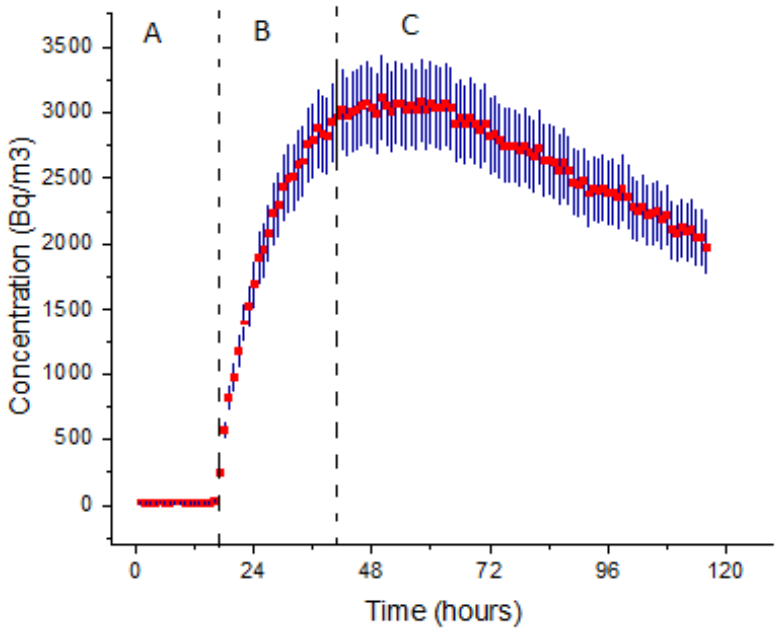

Figure 2.21: Radon concentration accumulation curve inside the closed chamber using a sample of water from San Giovanni in Fiore.

The temperature and humidity inside the chamber was monitored and retrieved from the Ecowitt data logger which indicated that it varied between 25.8 ^{o}C and 24.3 ^{o}C with an average of 25 ± 0.4 ^{o}C. The Ostwald coefficient was calculated and held constant at 0.22, since the variation in the constant is low for these small temperature changes. The relative humidity inside the chamber at the beginning of the experiment was 44% reaching 99% in the last two days of measurements.

The described experiment provides all the parameters of the Equation (2.37). The radon activity concentration in the analyzed water sample obtained was 133 ± 7 Bq l^{-1}, value reported in Chapter 4, Table (4.7).

Chapter 3

Building materials radon exhalation rate

In the first section of this chapter are presented measurements results for the determination of the chambers leakage in both the IRL and NTL. The values obtained, together with the laboratory background of radon concentration, are relevant parameters for the calculation of the exhalation rate with the closed chamber techniques, presented in the second section. The samples investigated are commonly used as building materials in Italy or Ecuador.

The protocol used can contribute to the realization of a standardized protocol and has been tested with samples of tuff previously measured at the IRL and then sent to the NTL for new measurements with independent instrumentation and different climatic and environmental conditions. The comparison of the results are presented in Section (3.2.3).

In the last part of the chapter, the determination of the surface and mass exhalation rate obtained with the electrets technique is presented together with the evaluation of the effective dose and alpha index associated calculation.

3.1 Chambers leakage

IRL chamber leakage

The chamber leakage has been studied performing several independent tests. To enrich with radon gas the chamber, at least with a concentration of 100 Bq m^{-3}, samples of tuff or water, sealed in the chamber for several days, has been used. The procedure is described in Section (2.2.2). The measurement

were performed measuring with one-hour intervals for about 7 days.

Table (3.1) and Figure (3.1) summarize the main leakage results obtained in the 2017-2019 period. The first column shows the year in which the experiment was performed and the two groups of four columns listing the leakage (λ_l), the total uncertainties, the $\chi^2/ndof$ of the fits and the Air Change Rate (ACR), defined as the product of λ_l and the chamber net volume (119 l $\pm$ 1%). The first group of data, named global fit, are the results of a fit to the function (2.6) were λ_l was a free parameter and the second group, named linear fit, shows the results obtained using the parameters obtained from the linear fit in equation (2.11). The results were obtained using tuff samples with the exception of the last two 2019 results obtained with water samples. As seen in Section (2.2.2), the concentration in the laboratory varies up to 40% during the winter with respect to the summer, for this reason, for both fits, the background radon concentration in laboratory (C_{bg}) used was obtained by dedicated measurements in the days preceding the experiment.

	Global fit (2.6)				**Linear fit (2.11)**			
Year	$\boldsymbol{\lambda_l}$ h^{-1}	**Uncer.** h^{-1}	$\boldsymbol{\chi^2/ndof}$	**ACR** $l\ h^{-1}$	$\boldsymbol{\lambda_l}$ h^{-1}	**Uncer.** h^{-1}	$\boldsymbol{\chi^2/ndof}$	**ACR** $l\ h^{-1}$
2017	0.00239	0.00026	2.6	0.28	0.00286	0.00154	5.2	0.34
2018	0.00072	0.00004	2.6	0.09	0.00085	0.00043	1.8	0.10
2019	0.00120	0.00002	2.1	0.14	0.00024	0.00012	2.4	0.03
2019	0.00067	0.00003	1.4	0.08	0.00014	0.00030	1.3	0.02
2019	0.00103	0.00003	1.6	0.12	0.00089	0.00031	1.1	0.11
2019	0.00088	0.00004	1.7	0.10	0.00062	0.00029	2.1	0.07

Table 3.1: IRL chamber leakage extracted from a global and a linear fit procedures, details are given in the text.

The results obtained with the global and linear fit procedures are slightly compatible. In all cases, the global fit is the most accurate. The first result in the table has been obtained with the standard protocol used by the group till 2016 and, comparing the results with the average value, reported in 2016 (0.00230 $\pm$ 4%) [34] a very good agreement is observed. The improvement of the sealing procedure, from 2018, obtained by wrapping the chamber in a plastic film, significantly reduced the leakage of the chamber, now well compatible or better than that found in the literature for similar apparatuses (see for example[50, 63, 64]).

About the differences between results in 2019, this is due to the method of closing the chamber which is conditioned by the force with which the lid

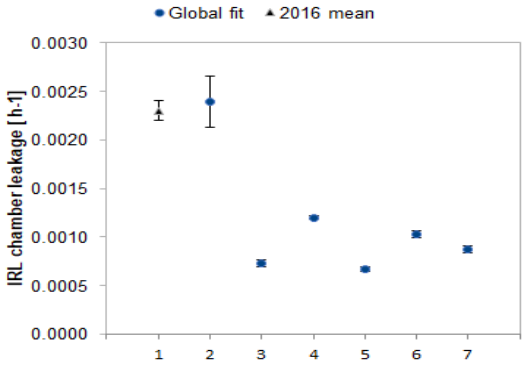

Figure 3.1: Table 3.1 results.

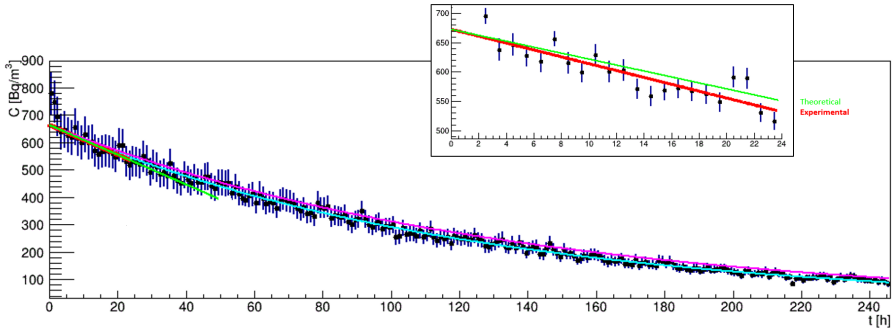

Figure 3.2: IRL chamber leakage test.

is screwed. An improvement in the closing technique is planned.

Figure (3.2) shows the leakage curve of the fourth result in Table (3.1). The light blue curve shows the global fit result, the pink curve the expected result assuming no leakage. The insert shows in red the linear fit result applied to the first 24 hours, the green line indicates the expected result assuming no leakage.

As is visible in the figure, particular attention was needed for the first 2-3 hours measurements, using the CPRD in particular. To reduce the time needed to remove the tuff sample, between the enriching and measuring phases, the detector was inserted at the beginning of the accumulation. In the first hours of the leakage study, the air in the CPRD still contains the higher radon concentration of the accumulation phase, few hours were needed for a complete equilibrium between the concentration in the CPRD and that

in the chamber, this effect can be observed in Figure (3.2) and Figure (2.11) where the first three data (3 hours) are particularly high. The fit procedure excludes the first few hours to avoid an overestimation of C_i.

In general, the linear fit provides less stable and precise results, the quality of the result is conditioned by the initial concentration obtained by enriching the chamber and has the only advantage of a limited period of time for the calculation, only 24h. The quality and stability of the global fit are much higher even if at least a week of measurements is necessary. For these reasons, we decided to use the leakage values obtained from the global fit for the extraction of the exhalation rate.

NTL chamber leakage

Applying the same procedure adopted at IRL, two independent experiments were performed at NTL (both with the chamber covered with a plastic film). Table (3.2) shows the results.

	Global fit (2.6)				**Linear fit (2.11)**			
Year	λ_l h^{-1}	**Uncer.** %	$\chi^2/ndof$	**ACR** $l\,h^{-1}$	λ_l h^{-1}	**Uncer.** %	$\chi^2/ndof$	**ACR** $l\,h^{-1}$
2018	0.00744	6	2.5	0.92	0.00893	12	5.9	1.11
2018	0.00225	5	1.1	0.28	0.00286	30	2.5	0.35

Table 3.2: NTL chamber leakage extracted from a global and a linear fit procedures, details are given in the text.

The first result in Table (3.2) shows a higher leakage due to a sealing technical problem for the lid of the chamber, solving the problem the air leakage has been greatly reduced.

At NTL, compatibility between results obtained with global and linear fit methods was observed. The Air Change Rate(ACR) has been calculated in each test, using a net volume of the chamber (124 l).

The second test reported in Table (3.2) is also shown in Figure (3.3). The light blue curve shows the global fit result, the pink curve the expected result assuming no leakage. The insert shows in red the linear fit result applied to the first 24 hours, the green line indicates the expected result assuming no leakage.

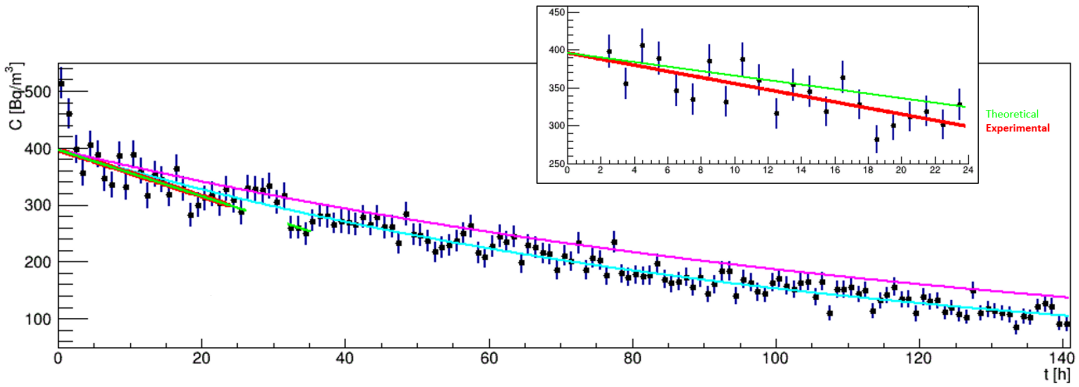

Figure 3.3: NTL chamber leakage test.

3.2 Radon exhalation rates using the closed chamber technique

3.2.1 Mass exhalation rate from Italian building materials

A large number of samples have been studied with the closed chamber technique to evaluate of the mass exhalation rate, most of the samples are Italian volcanic tuff samples, some of these coming from constructions under renovation, in all cases the extraction cave is not known, details on the samples are in Section (2.2.1), and Table (2.2).

Sample	**Global fit**			**Linear fit**		
	E_0 Bq kg^{-1} h^{-1}	Uncer. %	χ^2/ndof	E_0 Bq kg^{-1} h^{-1}	Uncer. %	χ^2/ndof
Gray 1 tuff	0.51	1	3.7	0.49	2	2.2
Gray 3 tuff	0.50	2	2.2	0.51	4	2.1
Gray 2 tuff	0.49	17	1.3	0.44	3	1.3
Yellow 2 tuff	0.48	2	1.4	0.44	4	1.6
Green 2 tuff	0.43	2	2.4	0.41	5	1.7
Yellow 1 tuff	0.33	2	1.6	0.32	4	1.3
Green 1 tuff	0.31	2	3.9	0.34	3	1.6
Gray 3 tuff (crushed)	0.51	24	1.5	0.47	16	0.9
Gray 1a tuff (crushed)	0.88	6	1.5	0.84	5	1.3
Gray 1b tuff (crushed)	0.84	2	1.6	0.86	7	1.8
Red granite	0.035	5	1.6	0.033	12	1.1
Sand	BDL			BDL		
Phosphorite	BDL			BDL		
Porphyry	BDL			BDL		

Table 3.3: Results of the mass exhalation rate of Italian building materials.

Table (3.3) summarizes the results obtained with global and linear fit procedures. In particular, the global fit has been obtained fitting Equation (2.6) and the result named linear fit has been obtained using the slope of a linear fit to Equation (2.16). In the table together with the mass exhalation rate E_0 are shown the total uncertainties expressed in percentage and the reduced χ^2 of the fits. The main contribution to uncertainty is due to the difficulty of determining the volume of the sample and thus the net volume of the chamber.

Defining the limit of detection as the smallest amount of activity concentration at equilibrium produced by the sample that can be reliably distinguished from the background, samples whose equilibrium concentration was compatible, within two standard deviations, with the chamber background were considered to be below the detection limit (BDL)[65].

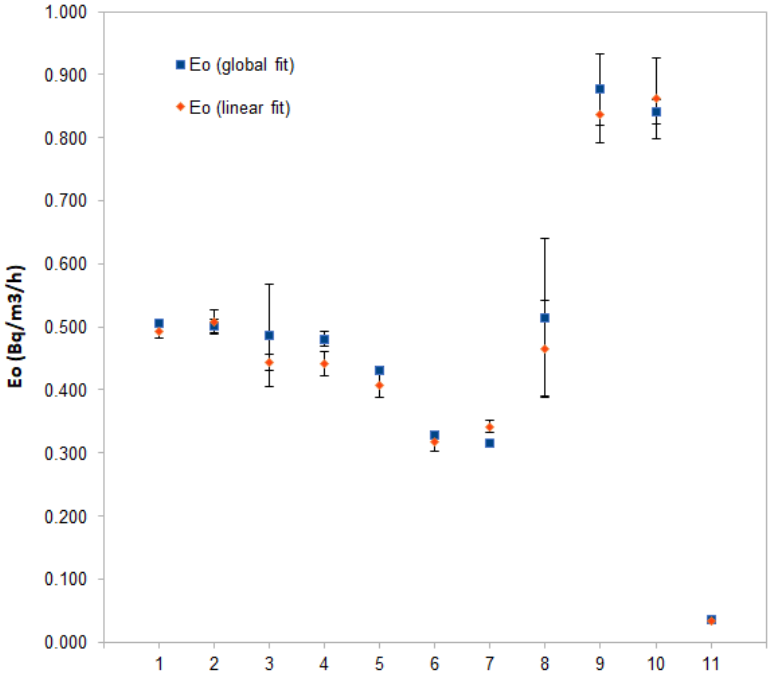

Figure 3.4: Table 3.3 results.

Comparing the two fit procedures, the results obtained were well compatible for almost all samples. Figure (3.4) shows the results presented in the Table (3.3) with their uncertainty. The values obtained with the global fit are, in most cases, higher than those obtained by the linear fit. A possible explanation may be linked to an underestimation of the effect of back diffusion or, more in general, to an overestimation of the equilibrium concentration if

extracted from the global fit.

There is an important difference, in terms of measurement time, between the two methods. In particular, at least 2-3 weeks are necessary to reach concentration equilibrium and to extract E_0, while 24 hours are enough to obtain results from the linear fit. Consequently, the linear fit is preferable, both because the low measurement time makes it easily usable even in extensive measurement campaigns, and because the effect of back diffusion is negligible in the first hours of measurement.

The large differences in terms of exhalation between samples are due to the different radium content in the samples but also a different materials porosity, permeability and emanation power. In particular, the mass exhalation rate of the solid tuff samples (linear fit) ranges from 0.32 to 0.51 Bq kg^{-1} h^{-1}.

The crushed tuff samples were placed inside the chamber in a rectangular glass container. For Gray 1a and 1b samples, a higher exhalation rate was observed than that obtained with the original sample and regardless of thickness. The exhalation of the sample Gray 3 crushed is well compatible with the result of the same sample not crushed. The main difference between the crushed samples Gray 1 and Gray 3 is the grain size which is respectively less than 1mm and between 1 and 8mm.

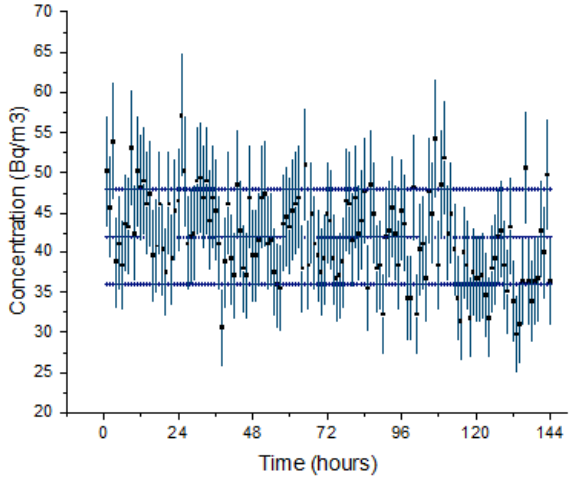

Figure 3.5: Radon concentration inside the chamber with a porphyry sample.

The samples of sand, phosphorite and porphyry showed very low accumulation of radon inside the chamber. The typical trend of the background concentration measurements inside the IRL chamber was observed for these samples. In Figure (3.5) the radon concentration measurement inside the chamber with the porphyry sample is shown.

3.2.2 Mass exhalation rate from Ecuadorian building materials

The mass exhalation rate of building materials of Ecuador performed at NTL and using a different detector (RAD7) are shown in Table (3.4).

Sample	**Global fit**			**Linear fit**		
	E_0 Bq kg^{-1} h^{-1}	Uncer. %	χ^2/ndof	E_0 Bq kg^{-1} h^{-1}	Uncer. %	χ^2/ndof
Concrete (home 1)	0.099	14	1.0	0.091	5	1.0
Concrete (home 2)	0.046	4	0.8	0.036	11	0.8
Granite A	0.095	5	1.0	0.081	10	1.1
Granite B	BDL			BDL		
Block 1	BDL			BDL		
Block 2	0.041	10	0.7	0.029	10	0.9
Brick 1	BDL			BDL		
Brick 2	BDL			BDL		
Brick 3	BDL			BDL		
Pozzolan	BDL			BDL		
Decorative stone	BDL			BDL		

Table 3.4: Mass exhalation rate of building materials of Ecuador.

The two concrete samples show a great difference in terms of exhalation, since they were made by mixing cement, sand, gravel and water, the different origin of the components used for mixing is probably the reason for the different results.

The two granite samples show different exhalation rate, they are different in colors and mix of minerals, (see in Figure (2.8)). The sample of granite B, shows an exhalation rate compatible with laboratory background, the same conclusion has been obtained for the block 1, the three brick samples, pozzolan and decorative stone of the Chimborazo volcano.

The mass exhalation rate of block 2 was similar to concrete (home 2), but less than the concrete (home 1) and granite A samples.

3.2.3 Comparison between laboratories measurements

As mentioned above, a laboratory, similar to the IRL, has been established at ESPOCH. In 2018, I conducted tests to validate the NTL camera and at the same time the protocol adopted in Italy.

The two laboratories are located in very different geographical areas and with a different environmental context. The IRL and NTL chambers have built with different materials but with the same gross volume, 125 liters. The sealing technique of the chambers is different. The characterization of the closed chambers in terms of leakage and background have been performed in the respective laboratories where the chambers are located. The net volume of the Ecuadorian chamber is slightly bigger to respect to the Italian chamber thanks to the fact that the detector is external to the chamber. The samples used for the tests in Ecuador were Gray 3 and Yellow 2, already measured at IRL.

Table (3.5) presents the results of mass radon exhalation rates from samples of Italian volcanic tuff and the name of the laboratory where the measurement was conducted.

The results are in very good agreement, both in terms of comparison between the two fit methods, one time more confirmed, than in terms of comparison between the results obtained with the same sample studied at different time, location, environmental conditions and with different detectors. The excellent agreement not only validates chambers and instrumentation adopted but also confirm that a comparison of the results is possible if a common detailed protocol is used.

Sample/detector	**Global fit**			**Linear fit**			**Laboratory**
	E_0 Bq kg^{-1} h^{-1}	Uncer. %	χ^2/ndof	E_0 Bq kg^{-1} h^{-1}	Uncer. %	χ^2/ndof	
Gray 3/RAD 7	0.50	2	1.3	0.48	3	0.7	NTL[1]
Gray 3/CPRD	0.50	2	2.2	0.51	4	2.1	IRL[2]
Yellow 2/RAD 7	0.52	3	1.0	0.45	4	1.0	NTL
Yellow 2/CPRD	0.48	2	1.4	0.44	4	1.6	IRL

[1] Nuclear Techniques Laboratory (Ecuador)
[2] Ionizing Radiation Laboratory (Italy)

Table 3.5: Mass exhalation rate from Italian tuff measured in Italy and Ecuador.

It should also be notice that for the test with sample Gray 3 conducted in Ecuador with RAD7 it was observed that, after 105 hours of monitoring, the

humidity inside the closed chamber increased from 3% to 18% and the temperature increased from 23.9 °C to 24.5°C for 44 hours. After this period, the humidity remained constant (18%), the temperature decreased to the initial value and also remained constant. This range of variations of temperature and humidity inside the closed chamber did not affect the results.

3.3 Radon exhalation rates using the electrets technique

The results of the exploratory study of the radon exhalation rate, using the electret ion chamber technique, are presented in Table (3.6). It shows the time interval of the measurements, and the surface and mass exhalation rate. The main sources of the total uncertainty is related to measuring time.

Sample	Δ**t**	E_0	Uncer.	E_0	Uncer.
	d	(Bq m^{-2} h^{-1})	%	(Bq kg^{-1} h^{-1})	%
White granite	7	0.07	32	0.004	32
Yellow 3 tuff	7	1.21	7	0.14	6
Gray 3 tuff (crushed)	3	3.92	9	0.39	9
Gray 1 tuff (crushed)	1	6.76	29	0.67	28
Gray 1 tuff (crushed)	3	7.05	7	0.70	7

Table 3.6: Radon surface and mass exhalation rate results, using the electrets technique.

The samples were tested with a time of accumulation of at least three days, except the sample Gray 1 tested with accumulation time of 1 and 3 days. As expected, a greater accumulation time gives a lower uncertainty in terms of radon concentration. Hence, special attention on the measurement period is recommended.

Knowing the rate of exhalation per unit of surface of a material, it is possible to estimate how much this will contribute to the indoor concentration of a possible room that could be built using that material.

As an example the Gray 1 and Gray 3 samples and the exhalation values reported in Table (3.6) have been used.

According with [66, 67], the contribution of building materials to the indoor concentration C_{Rn} can be calculated as follows:

$$C_{Rn} = \frac{E_0\ S}{V\ (\lambda_{Rn} + \lambda_v)} \tag{3.1}$$

where E_0 is the surface exhalation rate (Bq $m^{-2}h^{-1}$), S is the surface of the room covered with a material exhaling radon, V is the net room volume and λ_v is the air removal rate (h^{-1}). Assuming the room as a cavity with S/V=2.0 m^{-1} and an air exchange rate of 0.5 h^{-1}, the annual effective dose can be calculated.

Using surface exhalation of the samples Gray 3 and Gray 1 (Δt =3 days) and assuming 7000 hours per year, the effective dose expected for the room simulated is 0.73 ± 0.07 mSv y^{-1} and 1.30 ± 0.11 mSv y^{-1} respectively.

The crushed samples of tuff in Table (2.2) were used to calculate the alpha index (see Section (1.3.1)). The specific activity of ^{226}Ra, determined using gamma ray spectrometry, is shown in Table (3.7) together with the index.

Sample	Weight	^{226}**Ra**	**Uncertainty**	I_α
	kg	Bq kg^{-1}	Bq kg^{-1}	
Gray 1	0.943	269.49	8.99	1.35
Gray 3	0.539	260.26	8.65	1.30

Table 3.7: Activity concentrations of ^{226}Ra and alpha index of samples of Italian tuff.

The values observed for the alpha index, are greater than one, for both samples of tuff. In this context, the Italian tuff could be considered a material of interest from the point of view of radiological protection.

3.4 Discussion on results

This study focuses on the advantages and disadvantages of the measurement techniques, most used in the literature, on the evaluation of the exhalation rate of commonly used building materials and, at the same time, aims to contribute to a possible and necessary measurement protocol. Radon exhalation rate databases of building material, extracted with different protocols

and measurement techniques, are available (see for example [68]), they show a low homogeneity of the information and therefore a low possibility to use the published results. An international standard protocol, not yet available, is clearly necessary.

Most of the samples analysed consists of volcanic tuff, the choice of this material is due to its wide use in Italy [69] but also because, being highly porous and inhomogeneous, it is able to highlight possible limits of the measurement techniques investigated. Some other samples were chosen for the low expected exhalation rate.

One of the parameters to be considered relevant, in closed chamber measurements, is the chamber leakage. The closed chambers built in the IRL and NTL laboratories, thanks to the improvements implemented, have a very limited leakage, to respect to the first tests [34] and are well compatible or better of the values published (see for example [50, 70, 63]. In particular, at IRL the leakage is lower than a corresponding ACR $0.15 \pm 1\%$ l/h or a daily change of air in the chamber per day of about 3%.

The chamber at the NTL has an air exchange per day of about 6%, the chamber optimization is still in progress, and the first tests performed during the 8 months spent at the ESPOCH University, during the second year of my Ph.D are encouraging. Further improvements to the tightness of the NTL chamber are under study, such as better insulation of the connectors between the chamber and the external detector.

In this work the two most common methods of determining the leakage were used, in Tab 3.1 (Tab 3.2 for the NTL) the results of tests are summarized, the first test, in 2017 is in very good agreement with what is obtained in the past and also reported in [34], the tests from 2018 highlight the reduction of chamber leakage achieved by improving the chamber tightness.

The technique called global fit extracts the result directly from the fit. In this case, the required measurement period is greater than about one day (needed for the linear fit method) and also depends on the initial and final concentration in the closed chamber. Furthermore, for both techniques an important parameter is the radon gas concentration background that is in the laboratory where the chamber is located. Once again, the comparison with other published works is difficult due to the modest dealing of the problem. The studies described in Section (2.2.2), as expected, show the seasonal variability of the background (up to 40% higher in winter than in summer)

and the day/night effect. For these reasons it is considered appropriate to perform a measurement of the laboratory background during the days before the leakage measurement. Alternatively, the average annual concentration in the IRL or the average concentration in the period May-August 2018 in the NTL can be used, resulting in a value of 41 $\pm$ 1 Bq m^{-3} and 28 $\pm$ 6 Bq m^{-3} respectively. The use of the average annual value of the background can significantly increase the uncertainty about the result.

Our protocol includes a leakage measurement of several days, using a global fit, each time a change in radon chamber performance is expected and at least once a year and a dedicated measurement of the background of the laboratory in which the chamber is located in the days leading up to the experiment.

In Tables (3.3) and (3.4), the results of the calculation of the exhalation rate were summarized, once again it was possible to compare the results obtained using the main methods described in literature for measurements in closed chamber. The results are in good agreement with both methods. However, the absence of back diffusion effects with the linear fit and the difference in terms of time required for each measurement, at least two to three weeks for the global fit and about one day for the linear fit, make the second technique preferable to the first. The linear fit method was therefore chosen for our protocol.

The radon mass exhalation rate of the samples of building materials tested varies from 0.04, for red granite, to 0.88 Bq $kg^{-1}h^{-1}$ for Gray 1a crushed tuff sample. Samples of sand, phosphorite, porphyry, brick, granite B, pozzolan and decorative stone from Chimborazo volcano, are considered below the measurement detection limit.

To investigate the influence of particle size on radon exhalation rates and to measure the 226-radium specific activity, two samples have been crushed. The crushed sample Gray 3 grain size was between 1 and 8 mm for 70% of the mass, the size of remnant less than 1mm. Part of the sample Gray 1 was also crushed, the grain size of the two crushed subsamples Gray 1 obtained was less than 1mm. For the first sample, the exhalation rate was comparable with the original sample but with greater uncertainty, for the other samples, Gray 1, the exhalation rate was clearly higher, this behavior is in agreement with what observed in [63] and related with the density of the material, further studies are planned. From the point of view of the protocol, information on the parameters on which the exhalation depends must be included, among

these there is surely the density of the measured sample and the grain size if crushed.

To test the protocol, two tuff samples has been transferred from IRL to NTL and measured exactly following the measurement protocol used at IRL. Although the environmental and experimental conditions were strongly different an excellent agreement has been obtained and reported in Table (3.5).

In addition, exploratory measurements using the electrec technique were made using samples with different exhalation rates. The two samples (White granite and Yellow 3) with low exhalation required a measurement time of one week. The tuff samples, with the highest exhalation rate, were measured for one or three days. The results are compatible with what was obtained with the closed chamber technique. However, despite the practical advantage and the economic cost of the method, it is definitely an important disadvantage that it is impossible to establish the measurement times necessary to obtain a result with limited uncertainty. The effective dose, calculated using the surface exhalation rate ((Δt =3 days) of the samples of crushed tuff Gray 3 and Gray 1 were 0.73 mSv y^{-1} and 1.30 mSv y^{-1} respectively.

The alpha index calculated for the samples of crushed tuff Gray 1 and Gray 3 was greater than 1, with radium activity concentrations that exceed the recommended upper limit in building materials (200 Bq kg^{-1}) as suggested by Radiation Protection Authorities [27]. It is possible that the radon exhalation from this material could cause indoor radon concentrations exceeding 200 Bq m^{-3}. The use of the alpha index for risk assessment can be an important overestimation of the problem as it is based only on the radio content in the material and not on the density and other properties of this. In addition, as seen in the table (3.3), the use of gamma spectrometry for the calculation of the index, requires the crushing of the sample by completely changing the available exhalation surface.

Chapter 4

Radon activity concentration measurements in water

Measurements of radon concentration in spring water were made using the same instrumentation as for the measurements of the exhalation rate and the protocol described in Section (2.3). In the first section will be shown the results obtained with the different instruments using samples from the fountain of Orbo, in Calabria. A collection of the results obtained from deep sources in Calabria and the province of Chimborazo is shown in the following two sections.

An official intercomparison between laboratories, organized by the ARPACAL E. Majorana laboratory, the only Italian laboratory certified for radon concentration measurements in spring water, it was held in November 2019. The IRL participated, carrying out measurements with electrets and closed chamber technique. Details of the intercomparison are presented in Section (4.4).

4.1 Radon concentration measurements at Orbo spring

This section presents a comparison among techniques and instruments used for measurements of the radon concentration in groundwater. The techniques compared are: the emanometric technique with Lucas scintillation cells or a solid state detector, gamma spectrometry, electret technique and radon chamber technique, presented in Section (2.3). For this purpose, water samples collected from Orbo spring (Figure (4.1)) have been used.

Figure 4.1: Different views of the Orbo spring, Castiglione Cosentino, Calabria region, Italy.

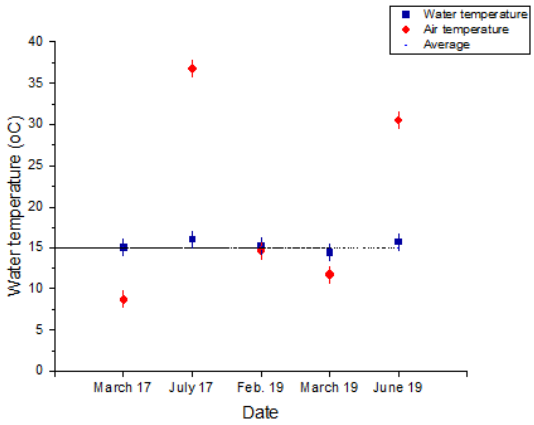

Figure 4.2: Orbo water temperature and air temperature in situ monitored during the 2017-2019 period.

The Orbo spring is public fountain with medium-high activity concentration, for this reason it can be considered a good reference source for the comparison between measurement techniques. Figure (4.2) illustrates the water and air temperatures in Orbo measured in the 2017-2019 period. Air temperature shows a wide seasonal variability, while the water temperature presents a limited range of variability. The mean water temperature in Orbo spring is $15 \pm 1\ ^{o}$C.

The water flow in the Orbo spring fluctuates between 3.7 ± 0.1 l/min (dry season) and 5.1 ± 0.5 l/min (rainy season).The increase in the water flow in the rainy season, could be due to the recharge of the aquifer with the water of the precipitations (rain, snow).

Date	**Instrumentation**	**Concentration (Bq l^{-1})**
August 2011 - March 2012	Lucas cell + Pylon degassing system	58 ± 4
November 2011	Gamma spectrometry	59 ± 2
March - August 2015	RAD7 + $RADH_2O$	62 ± 4
November 2015	Lucas cell + closed chamber	58 ± 3
February - August 2016	Lucas cell + H2O kit	63 ± 3
July 2016	Lucas cell + closed chamber	58 ± 3
November 2016	Lucas cell + closed chamber	62 ± 5
October 2016	Gamma spectrometry	60 ± 2

Table 4.1: Historical registry of the average radon concentration of activity in water samples of the Orbo fountain, the measurement techniques and instrumentation are also reported.

At the beginning of my studies various measurements were already available for the Orbo spring since summer 2011. Table (4.1) shows the results of the measurements performed from August 2011 to October 2016 [34], [71]. The spring monitoring continued during the 2017-2019 period. The following tables show the results obtained in the period 2017-2019, arranged by technique.

Table (4.2) summarizes the average values of the radon concentration, in water samples of the Orbo spring, using the **emanometric technique**. The first result is in agreement with the measurements presented in Table (4.1), while in June 2017 a higher concentration was observed.

Date	Rn concentration Bq l^{-1}	Uncert. Bq l^{-1}	Instrumentation
March 2017	68	3	Lucas cell + H2O kit
July 2017	84	3	Lucas cell + H2O kit

Table 4.2: Radon concentration results obtained using emanometry.

In July 2017 a measurement has been performed also with the **electrets technique** and the same concentration has been observed, as reported in

Table (4.3). In the same table, there are two more measurements performed during the year 2019. The comparison of the results, as a function of time, indicates a change, with respect to the past, in the conditions of the aquifer during 2017.

Date	Rn concentration Bq l^{-1}	Uncert. Bq l^{-1}
July 2017	81	4
February-March 2019	74	4
June 2019	74	4

Table 4.3: Radon concentration using electrets.

The results obtained with the new technique available at IRL, the **closed chamber technique** using a CPRD detector, are particularly interesting and shown in Table (4.4). This technique is still under development, and the main contribute of total uncertainties includes the uncertainties associated with the water insertion procedure and the equilibrium time evaluation. The results are in agreement with the others results presented.

Date	Rn concentration Bq l^{-1}	Uncert. Bq l^{-1}
March 2017	62	4
February 2019	77	4
March 2019	73	4
November 2019	56	3

Table 4.4: Radon concentration using the closed chamber.

A single measurement, using **Gamma-ray spectrometry** has been executed at ARPACAL agency of Cosenza, in March 2019, the result, 59±4 Bq l^{-1} is compatible with the two results presented in Table (4.1) but it is lower than observed since mid-2017.

For the analyzed sample, the ^{226} Ra specific concentration was found negligible. It is an indication that the concentration of radon, measured in the water samples of the Orbo spring, is not due to the decay of ^{226} dissolved in water but by the direct emanation of radon from rocks, in which are present

the precursors of radon, in contact with groundwater.

To simplify the comparison, Table (4.5) summarizes the average radon activity concentration in water samples collected from Orbo spring, obtained during the three years of my Doctoral course. The results obtained in different periods, various detectors and techniques, show a good agreement. A temporary increase of the radon concentration, in the period July 2017 - June 2019, was observed except in the case of the measurement of March 2019 with gamma spectrometry. The measurements carried out in November 2019, using the electret and closed chamber techniques, appear to indicate that the radon concentration in water samples collected at Orbo spring, returned to the values presented in Table 4.1.

From the behavior of the results obtained, it can be concluded that periodic monitoring of natural springs is necessary also for those apparently stable over time.

Date	**Instrumentation**	**Rn concentration (Bq l^{-1})**
March 2017	Lucas cell + H2O kit	68 ± 3
March 2017	Lucas cell + closed chamber	62 ± 4
July 2017	Lucas cell + H2O kit	84 ± 3
July 2017	Electret + E-Perm kit	81 ± 4
February 2019	Electret + E-Perm kit	75 ± 4
February 2019	Lucas cell + closed chamber	77 ± 4
March 2019	Electret + E-Perm kit	74 ± 4
March 2019	Lucas cell + closed chamber	73 ± 4
March 2019	Gamma spectrometry	59 ± 4
June 2019	Electret + E-Perm kit	74 ± 4
November 2019	Lucas cell + closed chamber	56 ± 3
November 2019	Electret + E-Perm kit	62 ± 3

Table 4.5: Average radon activity concentration in water samples collected from Orbo spring using various measurement techniques.

.

The main differences between techniques in terms of performance for measurement campaigns are summarized in Table (4.6) where the lowest detection limit (LDL) and the time needed for a single measurement are reported.

The comparison among the techniques can be useful to evaluate the most suitable instrumentation during measurement campaigns of radon gas concentration in spring water. It was observed that the measurements carried

Technique	LDL Bq l^{-1}	Time h
Gamma spectrometry	10	72
Emanometry-RAD7	0.004	<1
Emanometry-Pylon	0.027	<1
Electrets	0.37	24
Radon chamber	0.037	48-72

Table 4.6: Overview of measurement techniques [72, 40, 37, 45, 39]

out with the emanometric technique are accurate and the short time needed for a measurement can be a real advantage to respect to the other techniques, however the degassing efficiency and the water characteristics (salinity, impurities, etc.) can significantly affect the results. The gamma spectrometry requires three days for a single measurement. The electret technique is accurate but, also in this case, a not negligible and variable measuring time is required depending on the water radon concentration. The new technique presented, uses a closed chamber that allows radon concentration measurement with results well compatible with the other standard techniques and is a promising alternative particularly interesting in the field of research on the dependency of the measurements from various environmental parameters as for example environmental temperature and humidity.

4.2 Results of radon concentration measurements in Calabria springs

A monitoring campaign is ongoing for various springs of the Calabria region, the sites monitored and results are presented in Table (4.7), in the chronological order in which springs were analyzed (March 2017 - November 2019 period), the instrumentation used is indicated in the last column. Orbo measurements, already presented, are not reported in the table. Measurements with gamma spectrometry was performed in collaboration with the Ing. G. Durante of the physics laboratory of the Cosenza Department of the ARPACAL (Agenzia Regionale per la Protezione dell'Ambiente della Calabria) within the framework of the scientific collaboration agreement between ARPACAL-UNICAL.

The concentrations in the springs varied from 0.8 to 148 Bq l^{-1}. All

Spring location	C_{Rn} **(Bq l^{-1})**	**Instrumentation**
San Fili/Piano Mulino	5.0± 0.4	Lucas cell + H2O kit
San Fili/Piano Mulino	4.5± 0.2	Gamma spectrometry
Fiumara	0.8± 0.2	Lucas cell + H2O kit
Melisa	3.2 ± 0.3*	Lucas cell + H2O kit
Roca di Neto	2.4 ± 0.2	Lucas cell + H2O kit
Fontana de Gardu/Torre Melisa	5.0 ± 0.4	Lucas cell + H2O kit
Bosco Parantoro	10.2 ± 0.6*	Lucas cell + H2O kit
Contrata Muri/Acri	2.9 ± 0.3	Lucas cell + H2O kit
Fontana degli amici/Luzzi	10.1 ± 0.6	Lucas cell + H2O kit
Fontana degli amici/Luzzi	14.7 ± 0.4	Gamma spectrometry
Matarese	4.8 ± 0.4	Lucas cell + H2O kit
Serra casino	11.7 ± 0.7*	Lucas cell + H2O kit
Contrata Marri	14.7 ± 0.8	Lucas cell + H2O kit
San Francesco	6.7 ± 0.5	Lucas cell + H2O kit
Pini	0.9 ± 0.2	Lucas cell + H2O kit
Mangia e bevi	14.9 ± 0.8	Lucas cell + H2O kit
Celico/Manneto	10.7± 0.8	Electret + E-Perm kit
Condofuri	12.5 ± 1.0*	Electret + E-Perm kit
Celico/Scarivaglione	8.3 ± 0.8*	Electret + E-Perm kit
Spezzano/Scarivaglione	2.9 ± 1.0*	Electret + E-Perm kit
Rossano/Fontana Cersa	32.6 ± 1.6	Electret + E-Perm kit
San Antonio	22.9 ± 1.4	Electret + E-Perm kit
San Giovanni in Fiore	148.2 ± 5.2	Electret + E-Perm kit
San Giovanni in Fiore	133.0 ± 7.0	Lucas cell + closed chamber

Table 4.7: Average radon activity concentration in water samples of Calabria springs, using various measurement techniques. * Single measure.

samples analyzed come from public sources of drinking water widely used by the population. The only spring of interest in terms of risk is the San Giovanni in Fiore spring (39°17'27.0"N 16°37'57.0"E), along the SS107 road and in the middle of the Sila massif. The area of San Giovanni in Fiore is rich in granites, Studies of indoor concentration in the houses of San Giovanni in Fiore, made with local material containing granite, show a medium-high concentration.[73].

4.3 Results of radon concentration measurements in Chimborazo springs

Measurements of radon activity concentration in wells and springs of the province of Chimborazo were performed using the emanometric technique.

The experimental setup consisted of the RAD7 continuous monitor and Durridge RAD H2O Rn kit, see Section (2.3.3). Table (4.8) reports the name of the springs or wells, the radon activity concentration measured in the water samples. The study was conducted at the NTL in the period March-August 2018, during my stay at the Faculty of Science of the ESPOCH University.

Well or spring name	**Radon concentration (Bq l^{-1})**
Llio well 1	3.4± 0.3
Llio well 2	6.2± 0.7
Llio well 3	4.2± 0.5*
Llio well 4	4.4± 0.5*
Llio well 5	7.2± 1.2
Llio well 6	6.0± 0.8*
Llio well 7	6.2± 0.5*
San Pablo-EMAPAR	10.1± 1.3*
Mulachimbana-Calera	0.2 ± 0.07
Guayco-San Andrés	1.4 ± 0.8
UNACH well	1.3± 0.4*
ESPOCH well 1	3.3± 0.5*
ESPOCH well 2	2.0± 0.8
San Luis	4.5± 1.5*
Abras	1.7± 0.5
Santa Teresita	6.6± 0.4
Las fuentes	2.5± 0.6
Barrio espiritu santo	7.0± 0.5
Reserva fauna Chimborazo	7.1± 1.0*
Faldas del Chimborazo	8.9± 1.2
San Pablo	8.7± 0.3
San Gerardo	9.1± 0.7*

Table 4.8: Radon concentration of activity in water samples of Chimborazo springs and wells, using the emanometric technique. * Average value.

The results of radon concentration measurements varied between 0.2 and 10 Bq l^{-1}, with uncertainties from 35% to 13%. In particular, the values reported for the 7 wells of LLio and the spring of San Pablo were of great interest, because they constitute an important drinking water supply for the city of Riobamba, capital of the province of Chimborazo. Radon concentrations ranged from 3.4 to 10 Bq l^{-1}.

Mulachimbana and Guayco are drinking water supplies of the Calera-Shobol Pamba community and the Guano city, they presented low radon concentration 0.2 and 1.4 Bq l^{-1} respectively. Low concentrations were also observed for the UNACH and ESPOCH wells and the springs located in different towns of the province (the last nine results reported in Table (4.8).

4.4 Intercomparison among Calabrian laboratories

In November 2019, a radon in-field intercomparison for the activity concentration measurement in water samples was organized by the E. Majorana certified laboratory of the ARPACAL of Catanzaro. The following laboratories participated in the intercomparison: two private laboratories, one laboratory measured with liquid scintillation, another measured with the emanometric technique with the RAD7 detector and the IRL laboratory participated by using the closed chamber interfaced with the Pylon CPRD and electret technique. The intercomparison spring was the Orbo spring already presented in this chapter. All participants performed the sampling, with their own procedure.

The main objective for the IRL laboratory participation was linked to the possibility to test and validate the closed chamber technique and to test a not standard procedure with electrets respect to the results presented in Sections (4.1) and (4.2) (standard procedure).

IRL collected six water samples. One sample was analyzed using the standard E-perm detection system, consisting of a 4 liters glass jar with rubber sealing ring, 136 ml sample bottle with a screw cap with Teflon seal, an S-chamber and a short-term electret (SST). Four samples were analyzed using the non-standard procedure which differs from the standard because a commercial 3 liters glass jar and 155 ml, 235 ml and two 151 ml sampling bottles were used, together with the SST system. The concentration was calculated using the Equation (2.25) described in Section (2.3) with the corresponding correction factors in the volume of the vessel and sampling bottles. The sixth 1.5 liters sample was used for the measurement in the closed chamber.

The ARPACAL laboratory communicated the reference result of 52 $\pm$ 7

Bq l^{-1} (verbal n. 52506 12/11/2019). The IRL results are reported in the Table (4.9) and Figure (4.3). The uncertainty reported is twice the total error.

Sample number	Rn concentration	Uncertainty	Percentage	Technique
Bq l^{-1}	Bq l^{-1}			
1	72	7	10	Electret standard
2	57	6	11	Electret not standard
3	67	7	10	Electret not standard
4	60	6	10	Electret not standard
5	71	7	10	Electret not standard
6	56	6	11	Closed chamber

Table 4.9: IRL results of the ARPACAL Intercomparison 2019.

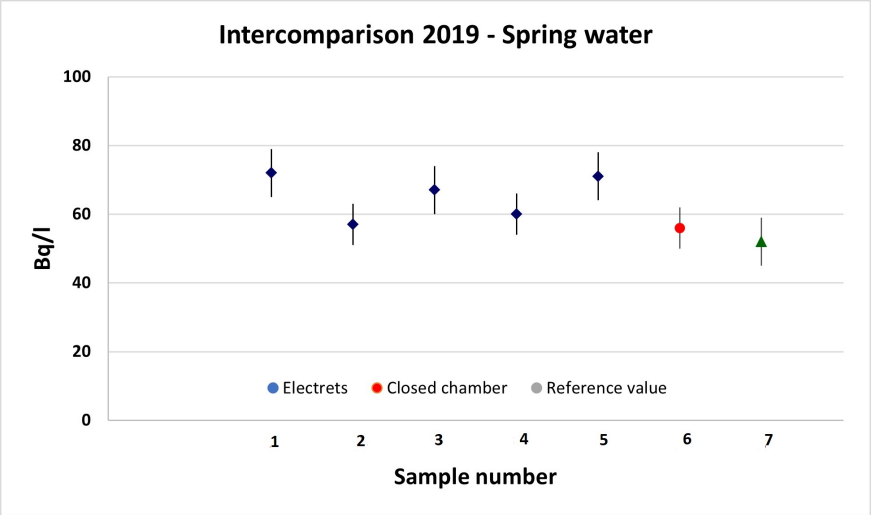

Figure 4.3: IRL results of radon concentration of activity in water samples of the Orbo spring - Intercomparison ARPACAL 2019.

The test performed, using the closed chamber, is in very good agreement with the reference measurement and confirms the quality of the chamber for this type of measurements. Measurements with the electret technique are compatible with the reference measurement. The 4 non-standard measurements are in agreement with the reference measurement.

4.5 Discussion on results

The monitoring of the Orbo spring, from summer 2011 to today, and its medium-high concentration, have allowed to consider it a reference spring

and made possible a comparison of the different performances of the four techniques presented in this study: emanometric, electrets, gamma spectrometry and closed chamber. All radon concentration measurements were made using the same sampling protocol as described in section (2.3.2). There is a good agreement between the techniques in measurements taken simultaneously. In addition, an increase in concentration was observed between 2017 and 2019, then returned to the typical value of the fountain, which confirms the need for periodic repetition of measurements.

From the ongoing monitoring of Calabrian springs, a concentration above 100 Bq l^{-1} was observed only in one public fountain out of the 22 studied, the San Giovanni in Fiore fountain, whose concentration, measured in a closed chamber, is 133.0 $\pm$ 7.0 Bq l^{-1}.

In the Chimborazo province, water samples from wells and springs that provide drinking water showed a radon concentration between 0.2 and 10 Bq l^{-1}. Wells and springs located in public places in the towns had concentrations from 1.7 to 9 Bq l^{-1}. The results of radon concentration in water samples from wells and springs studied in the province of Chimborazo are below the international reference levels for water intended for human consumption, therefore there is no health risk of the population.

The comparison between laboratories equipped with instruments for measuring the concentration of radon activity in water samples, using samples from the Orbo spring, confirmed the excellent performance of the closed chamber technique, with similar or better uncertainty than other commonly used techniques. This chamber will be useful for research activities, such as studies of the gas water/air transfer rate as a function of environmental parameters such as temperature and humidity. The chamber characterization is still ongoing.
In terms of measurement campaigns, the emanometric technique can certainly be taken into account, both for the quality of the measurements and for the relatively low costs and the relatively short measurement time.

Numerous Italian and Ecuadorian natural drinking water, were analyzed. In the IRL the measurements were made using the emanometric and closed chamber techniques in 2017 and the electret and closed chamber technique in the 2018-2019 period. In the NTL the measurements were made in the period March-August 2018, the emanometric technique was used. All measurements, both in the NTL and the IRL, have been performed with the same sampling and measurement protocols.

Chapter 5

RadioLab dissemination project

5.1 The project

RadioLab is a national project of the Istituto Nazionale di Fisica Nucleare (INFN), designed for scientific dissemination. The project is for high school students and most regions of Italy participate. The aim of the project is to integrate didactics with scientific communication and research on radioactivity, with special emphasis on the radon gas. Students are directly involved in laboratory activities, following the footsteps of researchers in the field and making measurements in their territory (schools but also homes or facilities considered by them of interest as far as radon risk is concerned). This project has immediate consequences in terms of dissemination of the contribution of the scientific approach to the assessment of the problem, social awareness, risk awareness, both for students and families and the society connected to them.

In the Calabria region the project manager is Professor Marcella Capua, with the collaboration of universities and INFN colleagues and myself. In particular, I was the coordinator of the laboratory measurements and the coordinator of the test project in Ecuador.

In Calabria the project is very ambitious, it has multiple objectives one of which is to teach students the scientific method and bring them closer to scientific research and their possible future as researchers. The project aims to fulfill the social role of science, that is, to protect and help the population, for example, health physics that is born from basic physics research and that has allowed great advances in diagnostic and treatment methods of diseases.

RadioLab intends to raise public awareness of the risk associated with radon, radioactive natural gas, present everywhere and easily measurable. Students among their activities in the project explain to the population the risk due to the presence of radon gas in their homes and workplaces. It is an integral part of the project, to conduct a series of interviews with the population, excluding relatives of students, on the perception of radon risk.

The project is articulated in three years cycles:

- In the first year students are introduced with seminars to: the main phases of the project and its objectives, the radon problem, radon concentration measurement techniques and national and international regulations and geological aspects of the Region. They organize events and conduct interviews, on the perception of radon risk,in different areas of the territory (markets, shopping centers, public squares, etc.) ; if the respondents declare that they do not know the problem, they offer them a brochure containing information about it, in Figure (5.1) the English version of the brochure is presented. Based on the information obtained from the seminars, the knowledge of the geological and social area in which they live, the students, choose public fountains and closed environments in which to make measurements in air and water of concentration of radon gas. All selected sites photographed and all informations are stored.

- In the second year, students learn more to radon measurement techniques, sampling and measurement protocols (common for all high schools). The INFN provides CR39 nuclear tracks detectors, and electrets. Students position and then withdraw the CR39 in homes (for approximately 6 months) and make measurements in spring water using electret following our instructions and described in Chapter 2.

- In the third year, the collected data are analyzed, discussed and compared between schools. The results of the measurements of the radon concentration in water and indoors are presented in a final Workshop, attended by schools, experts, authorities and the general public.

All three years, the students, organize events in which they carry out interviews and offer brochures to inform the population about the radon problem, the possible remedies and the importance of research and measurement. In particular, events were organized during the researchers' night, science festival and the international radon day on 7 November.

Figure 5.1: RadioLab brochure.

5.2 RadioLab cycle 2017-2019

In the 2017-2019 cycle, four schools from different areas of Calabria (Cosenza, Vibo Valentia, Soverato e Reggio Calabria) and 115 students participated.

Each school selected 9 houses or a public site and 16 fountains, performed 1530 interviews, offered more then 3000 brochure and organized or partecipated to Researcher Night 2018 and 2019, Radon Day 2017, 2018 and 2019, Vibo Valentia Festival of science 2018 and 2019 and the RadioLab summer schools 2018 [74] and 2019.

With regard to the results of the measurements, it should be noted that these are only exploratory measures carried out by students and with great uncertainties, however, in some cases, interesting results have been found that deserve further study. In particular, in a house in the province of Vibo Valentia and one in Reggio Calabria, radon concentrations over 500 Bq/m^3 were found and a sample of collected spring water in the Reggio Calabria area measured a radon concentration of 166 ± 5 Bq/l. Much of the results are in line with the findings of the experts in the relevant areas.

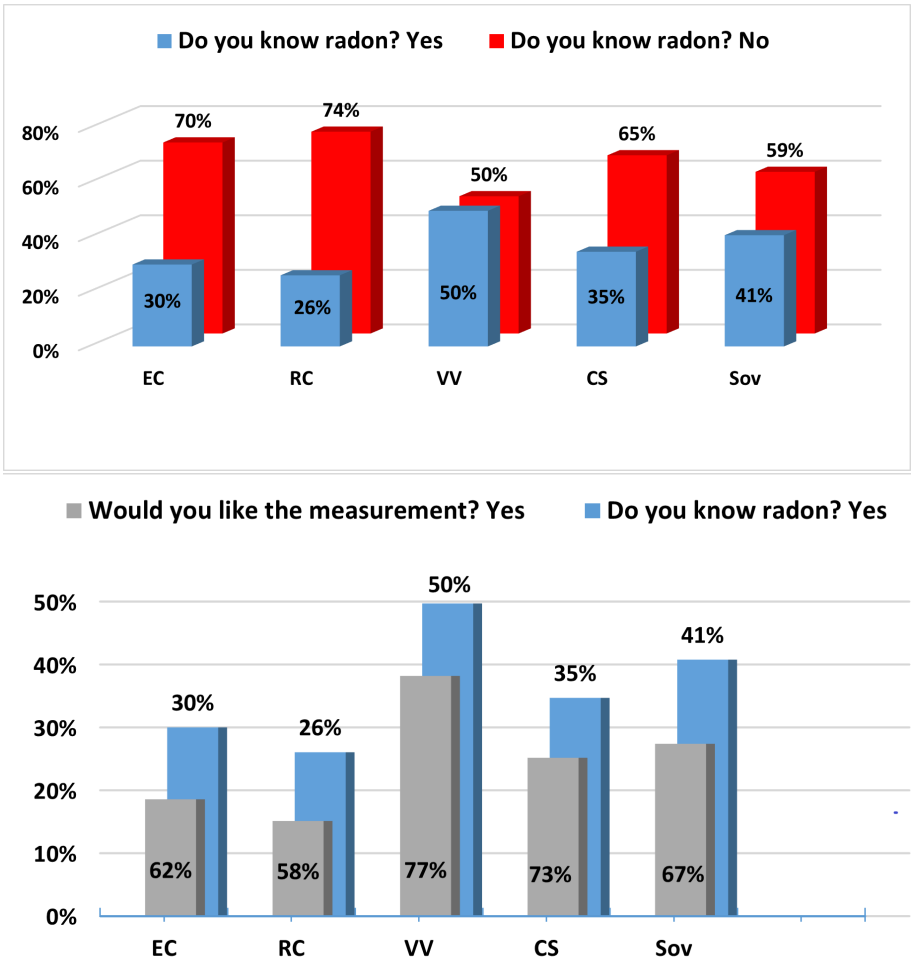

Figure 5.2: Interviews on the degree of knowledge of radon gas, performed by the students of the Radiolab project, see text for details.

As for the interviews, the results are interesting and in agreement with the socio-economic characteristics of the territory. Figure (5.2) shows, at the top, the answers to the question *Do you konw radon?* for the various areas covered with the interviews, in yellow the fraction of these interested to a possible measurements, in Ecuador and Reggio Calabria there is a lesser knowledge of the radon problem. The figure (5.2) at the bottom, shows the fraction of people interviewed and who declare to know radon, interested in the measures, also in this case, the inhabitants of Ecuador and Reggio Calabria would seem to be less available for measurements. Our observation is

in line with what the experts observed.

Figure (5.3) shows from the top left to the bottom right: a fantastic day of study outdoors during the 2018 Summer School on Monte Rosa; the event organized for Radon Day 2018 at the Fermi school in Cosenza, in which all 115 RadioLab students participated; the students of the project in front of the INFN stand during the night of the researchers 2019 at UNICAL: pairs of students alternated in different shifts, disguised as a bad radon and good scientist, the good scientist defended the guests of the researchers' night with a hammer from the dangerous radon, around the scene, other students conducted interviews or offered brochures; during the Science Festival 2018, the students organized a public meeting on the topic of radon and held a round table on the topic.

Figure 5.3: Pictures of events organized by students, see text for details.

The end-of-cycle workshop was organized in the main lecture hall at the University of Calabria, on November 7, 2019. Figure (5.4) shows the workshop poster.

The organization, registration, chairpersons and presentations were managed by the Calabrian and Ecuadorian students of RadioLab.

Figure 5.4: The Workshop 2019 poster.

In addition, after the presentations of the results by the students, two

interesting presentations have been added: Dr. S. Procopio of the Italian Regional Agency for the Protection of the Environment (ARPACAL) presented the state of the art on the knowledge of radon risk in Calabria and showed the good agreement with the student data and the importance of the diffusion of knowledge; Prof. G. Vingelli presented the first results of interviews on gender and STEM issues carried out even by the RadioLab students in 2019 and still ongoing. The event was attended by about 500 Calabrian students and about 100 personalities from the area (mayors, councilors, geologists, experts, professors, etc.) and was undoubtedly successful with repercussions also in the national press.

5.3 RadioLab test project for Ecuador

In the last year of the first cycle of the project, two high schools in Ecuador have collaborated to a pilot project of indoor measurements in the province of Chimborazo with the support of INFN RadioLab team and the University of Calabria. The training of the students was carried out remotely and with collegues of ESPOCH.

Taking into account the success of the pilot project, the coordinator in Calabria has decided to include the Ecuadorian group in the second cycle of RadioLab. It will be considered as the external group of the Calabrian project. This group will be coordinated by Professor Jheny Orbe, as an external partner.

The students participated in all the activities of the last year including the interviews and the organization and presentation at the workshop in which, a delegation of six students attended. In Figure (5.5) the delegation of Ecuadorian students, the Coordinator of Radiolab in Calabria, a Professor at ESPOCH, the Rector of a high school in Ecuador and myself.

Figure 5.5: Delegation of Ecuadorian students, Professor Marcela Capua, Professor Magdy Echeverría, Professor Edison Andrade and Professor Jheny Orbe.

Conclusions

This research presents the results of measures aimed at extracting the radon exhalation rate from building materials and the concentration of radon activity in the spring water, using Italian and Ecuadorian samples. The measurements were carried out at the IRL and NTL laboratories, equipped with similar instrumentation.

The main conclusions about building materials are summarized below:

The characterization of the IRL and NTL chambers was carried out with numerous tests, the leakage of the chambers produces an ACR of 0.14 l h^{-1} and 0.28 l h^{-1} at IRL and NTL, respectively. The NTL chamber needs better sealing procedures, already planned. It has also been shown that the background of the laboratory must be assessed just before the exhalation experiment, significantly reducing the uncertainties about exhalation.

In the literature two procedures for extracting the exhalation rate from closed chamber measurements are proposed. This work shows that the procedure that uses a linear fit over the first 24 hours of measurement is definitely preferable and is not affected by the effect of back diffusion.

Among the Italian building materials investigated, it shows that volcanic tuff samples have the highest mass exhalation rate with values ranging from 0.32 to 0.51 Bq kg^{-1} h^{-1}, the great differences in terms of exhalation between the samples are due to the different content of radium in the samples but also to a different porosity of the materials, density, permeability and emanating power.

Tests performed with crushed Italian tuff with grain size less than 1 mm, using the closed chamber and electret techniques, showed a mass exhalation rate clearly higher than the compact rock. The results confirm that the exhalation rate of the Italian tuff depends on the grain size of the sample and

then the porosity of the materials.

The building materials typically used in Ecuador and examined have an exhalation rate between 0.041 and 0.099 Bq kg $^{-1}$ h $^{-1}$. The maximum was in a concrete sample and the minimum in a block sample. A second concrete sample, whose components are of different origins, showed a lower exhalation rate (54 %) than the first sample.

Experiments carried out with Italian materials, using the electret technique, shown results on mass exhalation rate in agreement with what was obtained with the closed chamber technique. However, the closed chamber technique is preferable, due to the better performance in terms of the time needed for a single accurate measurement.

To test the new chamber in Ecuador, two tuff samples were transferred from Italy to NTL and measured exactly according to the measurement protocol used in Italy. The results of the exhalation rate are in excellent agreement with what has been obtained. The completely different environmental conditions and experimental contexts did not influence the exhalation rate of the materials.

The protocol used adds various requirements to what is indicated in the literature and contributes to the creation of an a standardized protocol for measuring the exhalation rate, extracted using the closed chamber technique.

Water Springs of the Calabria region in Italy and of the Chimborazo province in Ecuador was also investigated. The conclusions are detailed below:

The results of radon concentrations of activity of Calabrian springs showed great variability, but only one spring, San Giovanni in Fiore, presented a concentration higher than the reference level in the Italian law (DL 28/2016)) of 100 Bq l^{-1}.

Wells and springs that are drinking water supply of the cities of Riobamba, Guano, the community of Calera-Shobol Pamba and the ESPOCH and UNACH Universities; besides other springs open to the public, presented low radon levels, with respect to international reference levels for water intended for human consumption.

The comparison between the radon measurement techniques in spring wa-

ter (emanometric, electret, gamma spectrometry and closed chamber), using water samples from the Orbo source, located in northern Calabria, leads to the conclusion that the emanometric technique is preferable in measurement campaigns.

The closed chamber technique for water measurements, developed in the UNICAL Department of Physics, was evaluated by participating in the first inter-comparison between Calabrian laboratories organized by the Majorana certified laboratory of the ARPACAL of Catanzaro. An excellent agreement was obtained between the closed chamber measurement and the reference measurement. The confirmation of the goodness of the technique will allow us to use the chamber in research activities, on the mechanisms of radon exhalation from water to air, keeping environmental parameters under control.

The outreach activities carried out with 115 students from various Calabrian schools and 39 students from two schools in Ecuador, trained the students on the problems of radon risk, on measurement techniques, and possible remedies. The social role of this work was highlighted by students' interviews on risk perception. In some areas of Calabria, less than 30% of the interviewees are aware of the radon risk, the relevant laws and the importance of measurements.

Acknowledgments

My gratitude to Professor Marcella Capua for scientific support during the research and writing of this thesis. A fraternal thank you for promoting the transfer of knowledge and development of scientific research in Ecuador.

A sincere thanks to the INFN for the financial support for the scientific dissemination of the research results and to the ARPACAL laboratory of Cosenza and Dr. G. Durante in particular, for the measurements performed for me.

To the Escuela Superior Politécnica de Chimborazo in the person of Dr. Byron Vaca, Rector, for his unconditional support to carry out my Ph.D. studies. To the Eng. Hannibal Brito, Former Dean of the Faculty of Sciences, and to the Architect Irina Tinoco, Director of the Department of Physical Development of the ESPOCH, for their support in the adaptation and implementation of the Nuclear Techniques laboratory.

Thanks to my family, especially to my parents for being present at every stage of my life, giving me her support and blessing. To my son Marlon for encouraging my dreams. To my daughter Deyaneira, my life partner, for giving me the strength to overcome every difficulty and with her presence fill the void of distance.

This thesis I dedicate to my grandmother Carmen, who always waits for my return regardless of time and distance.

Jheny del Carmen Orbe Ordoñez
Università degli studenti della Calabria
November, 2020.

Bibliography

[1] Robert C Weast, Melvin J Astle, William H Beyer, et al. *CRC handbook of chemistry and physics*, volume 69. CRC press Boca Raton, FL, 1988.

[2] Uranium thorium and actinium decay series, https://researchgate.net/series-ojovan-and-lee-2005-fig5-303487529, lastchecked: 03.02.2020.

[3] Saeed A Durrani and Radomir Ilic. *Radon measurements by etched track detectors: applications in radiation protection, earth sciences and the environment*. World Scientific, 1997.

[4] William W Nazaroff. Radon transport from soil to air. *Reviews of Geophysics*, 30(2):137–160, 1992.

[5] Marvin Wilkening. *Radon in the Environment*, volume 40. Elsevier, 1990.

[6] Allan B Tanner. Radon migration in the ground: a supplementary review. *US Geological Survey Open-File Report*, 78(1050):61, 1978.

[7] WB Silker and DR Kalkwarf. Radon diffusion in candidate soils for covering uranium mill tailings. Technical report, Pacific Northwest Lab., Richland, WA (USA), 1983.

[8] Robert L Fleischer and Larry G Turner. Correlations of radon and carbon isotopic measurements with petroleum and natural gas at cement, oklahoma. *Geophysics*, 49(6):810–817, 1984.

[9] IP Dobrovolsky, SI Zubkov, and VI Miachkin. Estimation of the size of earthquake preparation zones. *Pure and Applied Geophysics*, 117(5):1025–1044, 1979.

[10] A Mogro-Campero and RL Fleischer. Subterrestrial fluid convection: a hypothesis for long-distance migration of radon within the earth. *Earth and Planetary Science Letters*, 34(2):321–325, 1977.

[11] William E Clements and Marvin H Wilkening. Atmospheric pressure effects on 222rn transport across the earth-air interface. *Journal of Geophysical Research*, 79(33):5025–5029, 1974.

[12] RL Fleischer. Permeability of caulking compounds to 222rn. *Health physics*, 62(1):91—95, January 1992.

[13] WJ Ward III, RL Fleischer, and A Mogro-Campero. Barrier technique for separate measurement of radon isotopes. *Review of Scientific Instruments*, 48(11):1440–1441, 1977.

[14] Katarzyna Walczak, Jerzy Olszewski, and Marek Zmyślony. of insulating building materials. *Nukleonika*, 61(3):289–293, 2016.

[15] Jing Chen and Leonora Marro. Assessment of radon equilibrium factor from distribution parameters of simultaneous radon and radon progeny measurements. *Radiation and environmental biophysics*, 50(4):597–601, 2011.

[16] National Research Council et al. *Risk assessment of radon in drinking water*. National Academies Press, 1999.

[17] Jay H. Lubin, Jr. Boice, John D., Christer Edling, Richard W. Hornung, Geoffrey R. Howe, Emil Kunz, Robert A. Kusiak, Howard I. Morrison, Edward P. Radford, Jonathan M. Samet, Margot Tirmarche, Alistair Woodward, Shu Xiang Yao, and Donald A. Pierce. Lung Cancer in Radon-Exposed Miners and Estimation of Risk From Indoor Exposure. *JNCI: Journal of the National Cancer Institute*, 87(11):817–827, 06 1995.

[18] Jonathan M Samet. Radiation and cancer risk: a continuing challenge for epidemiologists. In *Environmental health*, volume 10, page S4. BioMed Central, 2011.

[19] Sarah Darby, D Hill, A Auvinen, JM Barros-Dios, H Baysson, F Bochicchio, H Deo, R Falk, F Forastiere, M Hakama, et al. Radon in homes and risk of lung cancer: collaborative analysis of individual data from 13 european case-control studies. *Bmj*, 330(7485):223, 2005.

[20] Daniel Krewski, Jay H Lubin, Jan M Zielinski, Michael Alavanja, Vanessa S Catalan, R William Field, Judith B Klotz, Ernest G Létourneau, Charles F Lynch, Joseph I Lyon, et al. Residential radon and risk of lung cancer: a combined analysis of 7 north american case-control studies. *Epidemiology*, 16(2):137–145, 2005.

[21] Jay H Lubin, Zuo Yuan Wang, John D Boice, Zhao Yi Xu, William J Blot, Long De Wang, and Ruth A Kleinerman. Risk of lung cancer and residential radon in china: pooled results of two studies. *International Journal of Cancer*, 109(1):132–137, 2004.

[22] EC-European Commission et al. Radiological protection principles concerning the natural radioactivity of building materials. *Radiation Protection*, 112, 1999.

[23] Serena Righi and Luigi Bruzzi. Natural radioactivity and radon exhalation in building materials used in italian dwellings. *Journal of Environmental Radioactivity*, 88(2):158–170, 2006.

[24] L Xinwei, W Lingqing, J Xiaodan, Y Leipeng, and D Gelian. Specific activity and hazards of archeozoic-cambrian rock samples collected from the weibei area of shaanxi, china. *Radiation protection dosimetry*, 118(3):352–359, 2006.

[25] Nisha Sharma, Jaspal Singh, S Chinna Esakki, and RM Tripathi. A study of the natural radioactivity and radon exhalation rate in some cements used in india and its radiological significance. *Journal of Radiation Research and Applied Sciences*, 9(1):47–56, 2016.

[26] Radiation Protection Authority Norwegian et al. Naturally occurring radioactivity in the nordic countries. recommendations. 2000.

[27] Nordic. Naturally occurring radiation in the nordic countries-recommendations, reykjavik. flag-book series, 2000.

[28] *Council Directive 2013/59/EURATOM. Laying down basic safety standards for protection against the dangers arising from exposure to ionising radiation.* 2013.

[29] *Council Directive 2013/51/EURATOM. Laying down requirements for the protection of the health of the general public with regard to radioactive substances in water intended for human consumption.* 2013.

[30] *Decreto legistativo n. 28. Gazzeta ufficiale della Repubblica Italiana.* Number 55. 2016.

[31] Environmental Protection Agency. *National Primary Drinking Water Regulations; Radon-222*, volume 64. 1999.

[32] World Health Organization. *Guidelines of drinking water quality, third edition incorporating the first and second addenda*, volume 1. 2008.

[33] World Health Organization. *Guidelines of drinking water quality, fourth edition.* 2011.

[34] Tene Fernandez. *Environmental Radon Measurements using a closed chamber for building materials and water and a feasible program for Ecuador.* PhD thesis, Department of Pysics of UNICAL, 2016.

[35] Henry F Lucas. Improved low-level alpha-scintillation counter for radon. *Review of Scientific Instruments*, 28(9):680–683, 1957.

[36] H. F. Lucas and D. A. Woodward. Effect of long decay chains on the counting statistics in the analysis of radium224 and radon222. *Journal of Applied Physics*, 35(2):452–456, 1964.

[37] Pylon Electronic Incorporated. *Introduction manual for using Pylon model 110A and 300A Lucas cell whit the Pylon model AB-5. Revision 0*, 1989.

[38] Pylon Electronic Company Inc. *Pylon Model AB-5 Portable Radiation Monitor - Instruction Manual. Rev. 5*, 1993.

[39] Pylon Electronic Development Company ltd. *Continuous passive radon detector. Instruction Manual. Rev 0*, 1989.

[40] DURRIDGE Company Inc. *RAD7 Radon detector - User manual*, 2014.

[41] Mayeen Uddin Khandaker. High purity germanium detector in gamma-ray spectrometry. *International journal of Fundamental physical sciences*, 1(2):42–46, 2011.

[42] P Kotrappa, JC Dempsey, JR Hickey, and LR Stieff. An electret passive environmental 222rn monitor based on ionization measurement. *Health Physics*, 54(1):47–56, 1988.

[43] Rad Elec Inc. Radon measurement systems, https://www.radelec.com, lastchecked: 12.12.2019.

[44] P Kotrappa, JC Dempsey, RW Ramsey, and LR Stieff. A practical e-permtm (electret passive environmental radon monitor) system for indoor 222rn measurement. *Health Physics*, 58(4):461–467, 1990.

[45] P Kotrappa and WA Jester. Electret ion chamber radon monitors measure dissolved 222rn in water. *Health physics*, 64(4):397–405, 1993.

[46] P Kotrappa and F Stieff. Electret ion chambers (eic) to measure radon exhalation rates from building materials. In *Proceedings of the 2008 International Radon Symposium*, pages 1–8. Citeseer, 2008.

[47] NP Petropoulos, MJ Anagnostakis, and SE Simopoulos. Building materials radon exhalation rate: Erricca intercomparison exercise results. *Science of the total environment*, 272(1-3):109–118, 2001.

[48] United Nations Scientific Committee on the Effects of Atomic Radiation et al. Sources and effects of ionizing radiation, unscear report 2008. *Vol II. New York: United Nations, 20tl*, 2000.

[49] Instituto Nacional de Estadísticas y Censos. *Encuesta de edificaciones 2016*. INEC, 2017.

[50] Christopher YH Chao, Thomas CW Tung, Daniel WT Chan, and John Burnett. Determination of radon emanation and back diffusion characteristics of building materials in small chamber tests. *Building and Environment*, 32(4):355–362, 1997.

[51] CY Chao and TC Tung. Radon emanation of building material–impact of back diffusion and difference between one-dimensional and three-dimensional tests. *Health physics*, 76(6):675—681, June 1999.

[52] J Pinel, T Fearn, SC Darby, and JCH Miles. Seasonal correction factors for indoor radon measurements in the united kingdom. *Radiation Protection Dosimetry*, 58(2):127–132, 1995.

[53] Jonathan C H Miles. Temporal variation of radon levels in houses and implications for radon measurements strategies. *Radiation Protection Dosimetry*, 93(4):369–375, 2001.

[54] CEA/LNE-LNHB 2007. Nucleide - Lara library for gamma and alpha emissions, 2007.

[55] G Iovine, I Guagliardi, C Bruno, R Greco, A Tallarico, G Falcone, F Lucà, and G Buttafuoco. Soil-gas radon anomalies in three study areas of central-northern calabria (southern italy). *Natural Hazards*, 91(1):193–219, 2018.

[56] Ministero dei lavori pubblici. *Le sorgenti italiane elenco y descrizione*, volume VI. INEC, 1941.

[57] Gobierno Autónomo Descentralizado de la Provincia de Chimborazo. *Plan de desarroollo y ordenamiento territorial de Chimborazo*. 2015.

[58] N Burbano, S Becerra, and E Pasquel. *Introducción a la hidrogeología del Ecuador 2da. Edición.* INAMHI, 2015.

[59] Mi.am s.r.l. *H2O-Rn-Kit per misura radon in acqua*, 2015.

[60] Rad Elect Inc. *Radon in water - User manual, version 2.321*, 2014.

[61] Joash N Ongori, Robert Lindsay, and Mashinga J Mvelase. Radon transfer velocity at the water–air interface. *Applied Radiation and Isotopes*, 105:144–149, 2015.

[62] Michael Schubert, Albrecht Paschke, Eric Lieberman, and William C Burnett. Air–water partitioning of 222rn and its dependence on water temperature and salinity. *Environmental science & technology*, 46(7):3905–3911, 2012.

[63] P. Tuccimei, M. Moroni, and D. Norcia. Simultaneous determination of 222rn and 220rn exhalation rates from building materials used in central italy with accumulation chambers and a continuous solid state alpha detector: Influence of particle size, humidity and precursors concentration. *Applied Radiation and Isotopes*, 64(2):254 – 263, 2006.

[64] M Abo-Elmagd. Radon exhalation rates corrected for leakage and back diffusion–evaluation of radon chambers and radon sources with application to ceramic tile. *Journal of Radiation Research and Applied Sciences*, 7(4):390–398, 2014.

[65] Sam Keith, John R Doyle, Carolyn Harper, Moiz Mumtaz, Oscar Tarrago, David W Wohlers, Gary L Diamond, Mario Citra, and Lynn E Barber. Toxicological profile for radon. 2012.

[66] Jing Chen, Naureen M Rahman, and Ibrahim Abu Atiya. Radon exhalation from building materials for decorative use. *Journal of environmental radioactivity*, 101(4):317–322, 2010.

[67] William W Nazaroff and Anthony V Nero. Radon and its decay products in indoor air. 1988.

[68] R Trevisi, S Risica, C Nuccetelli, S Onisei, and F Leonardi. Natural radioactivity in building materials in the european union: a database of activity concentrations, radon emanations and radon exhalation rates. *Istituto Superiore di Sanità*, 2017.

[69] United Nations. Scientific Committee on the Effects of Atomic Radiation. *Effects of ionizing radiation: UNSCEAR 2006 Report to the General Assembly, with scientific annexes*, volume 2. United Nations Publications, 2009.

[70] Xing Lei, Lei Zhang, and Qiuju Guo. Comparison of closed methods for accurate measurements of radon exhalation rates from building materials. *Radiation Protection (Taiyuan)*, 31(1):13–16, 2011.

[71] Maria Chiara Angiocchi. Protocollo di misura e analisi dati di concentrazione di radon acqua, 2010/2011.

[72] Viktor Jobbagy, Timotheos Altzitzoglou, Petya Malo, Vesa Tanner, and Mikael Hult. A brief overview on radon measurements in drinking water. *Journal of environmental radioactivity*, 173:18–24, 2017.

[73] V Nastro, DL Carnì, A Vitale, F Lamonaca, and M Vasile. Passive and active methods for radon pollution measurements in historical heritage buildings. *Measurement*, 114:526–533, 2018.

[74] F Groppi, A Bazzocchi, S Manenti, J Immé, M Pugliese, V Fanti, M Capua, A Ventura, V Montalbano, M Chiosso, et al. Summer school del laboratorio radon per la scuola secondaria. In *104 Congresso Nazionale della Società Italiana di Fisica*, 2018.

Participation in conferences

The results collected in this thesis have been presented at the following Conferences:

- 7 Incontri Mediterranei di Igiene Industriale: Inquinamento Indoor e Outdoor: Valutazione dei Rischi, Figure e Competenze, 3 - 4 ottobre 2019, Lamezia Terme, Italy, Oral presentation: Radon risk in spring water, comparison between measurements techniques.
- 7 Incontri Mediterranei di Igiene Industriale: Inquinamento Indoor e Outdoor: Valutazione dei Rischi, Figure e Competenze, 3 - 4 ottobre 2019, Lamezia Terme, Italy, Oral presentation: Calcolo mediante camera chiusa del tasso di esalazione di gas radon in campioni di tufo italiano.
- ENVIRA 2019: 5th International Conference on Environmental Radioactivity, 8 - 13 September 2019, Prague – Czech Republic, Oral presentation: Comparison between measurements techniques of radon concentration in spring water.
- ENVIRA 2019: 5th International Conference on Environmental Radioactivity, 8 - 13 September 2019, Prague – Czech Republic, Oral presentation: Evaluation of the radon mass exhalation rate in Italian tuff using the closed chamber technique.
- ICRER 2019: 21th International Conference on Radioecology and Environmental Radioactivity, 20 - 21 June 2019, Vienna, Austria, Oral presentation: Radon exhalation rate measurements of Italian tuff with closed chamber technique.
- Convegno Nazionale AIRP di Radioprotezione, 8-10 Novembre 2017, Salerno – Italia, Poster: Misurazioni di concentrazioni di attività del gas radon in acqua ad uso pubblico nella Provincia di Cosenza. Un possibile protocollo regionale ad adempimento delD.Lgs. 15 febbraio 2016, n.28.

- Convegno Nazionale AIRP di Radioprotezione, 8-10 Novembre 2017, Salerno – Italia, Poster: Misure di rate di esalazione di gas radon in campioni di tufo laziale mediante camera chiusa.